UNIVERSITÀ
DEGLI STUDI
DI PADOVA

Università degli Studi di Padova

Dipartimento di MEDICINA - DIMED

CORSO DI DOTTORATO DI RICERCA IN SCIENZE CLINICHE E SPERIMENTALI

CURRICOLO IN SCIENZE REUMATOLOGICHE E LABORATORISTICHE

XXXII CICLO

Experimental thesis

Novel Pathogenic Pathways and Therapeutic Implications in Lupus Nephritis: The Emerging Role of PTX3-Related Immunity

Coordinatore: Ch.mo Prof. (nome e cognome)

Supervisore: Ch.mo Prof. Andrea Doria

Dottoranda: Dott.ssa Mariele Gatto

Table of contents

List of papers discussed in the thesis

Paper I

SERPINB3 Delays Glomerulonephritis and Attenuates the Lupus-Like Disease in Lupus Murine Models by Inducing a More Tolerogenic Immune Phenotype.

Gatto M, Luisetto R, Ghirardello A, Cavicchioli L, Codolo G, Biasiolo A, Maggioni G, Saccon F, Beggio M, Cappon A, Venturini R, Pontisso P, Doria A.

Frontiers Immunology 2018;9:2081.

Paper II

Immunization with pentraxin 3 (PTX3) leads to anti-PTX3 antibody production and delayed lupus-like nephritis in NZB/NZW F1 mice.

Gatto M, Ghirardello A, Luisetto R, Bassi N, Fedrigo M, Valente M, Valentino S, Del Prete D, Punzi L, Doria A.

Journal of Autoimmunity 2016;74:208-216

Paper III

Circulating Pentraxin3-Specific B Cells Are Decreased in Lupus Nephritis.

Gatto M, Wiedemann A, Nomovi N, Reiter K, Schrezenmeier E, Rose T, Szelinski F, Lino AC, Valentino S, Ghirardello A, Dörner T, Doria A.

Frontiers Immunology 2019;10:29.

Paper IV (unpublished)

Renal ultrastructural findings suggest immunization with PTX3 prevents transition from the preclinical to the clinical stages of lupus-like nephritis in NZB/WF1 mice: a microscopy-based study.

Gatto M, Radu C, Ghirardello A, Luisetto R, Bonsembiante F, Trez D, Valentino S, Simioni P, Cavicchioli L, Doria A.

Manuscript in preparation

Other papers (review articles, viewpoints) on the topic:

Clinical and pathologic considerations of the qualitative and quantitative aspects of lupus nephritogenic autoantibodies: A comprehensive review.

Gatto M, Iaccarino L, Ghirardello A, Punzi L, Doria A.

Journal of Autoimmunity 2016;69:1-11

PTX3, Anti-PTX3, and Anti-C1q Autoantibodies in Lupus Glomerulonephritis.

Bassi N, Del Prete D, Ghirardello A, Gatto M, Ceol M, Zen M, Bettio S, Mantovani A, Iaccarino L, Punzi L, Doria A.

Clinical Review in Allergy and Immunology 2015;49:217-26.

Serpins, immunity and autoimmunity: old molecules, new functions.

Gatto M, Iaccarino L, Ghirardello A, Bassi N, Pontisso P, Punzi L, Shoenfeld Y, Doria A.

Clinical Review in Allergy and Immunology 2013;45:267-80

Emerging and critical issues in the pathogenesis of lupus.

Gatto M, Zen M, Ghirardello A, Bettio S, Bassi N, Iaccarino L, Punzi L, Doria A.

Autoimmunity Reviews 2013;12:523-36

Nephritogenic-antinephritogenic antibody network in lupus glomerulonephritis.

Doria A, Gatto M.

Lupus 2012;21:1492-6

SUMMARY

Background. Abnormalities affecting regulatory molecules and pentraxin (PTX) 3 have been suggested to contribute to development of lupus glomerulonephritis (LN). Characterization of novel pathogenic pathways could pave the way to targeted therapeutic approaches.

Aims. To investigate the role and relevance of PTX3/anti-PTX3 related immunity in systemic lupus erythematosus (SLE) patients and in lupus murine models and to explore the *in vivo* effects of restoration of SERPINB3 levels.

Methods. The overall project comprised four experimental phases. Three out of four experiments were carried out on murine models of SLE, either New Zealand Black/White (NZB/W F1) or Mrl/lpr mice, while one experiment was conducted in humans.

In the first experiment, intraperitoneal administration of recombinant SERPINB3 (7.5 μg/0.1mL or 15 μg/0.1mL) or placebo (PBS 0.1 ml) was carried out in 40 NZB/W F1 mice divided into four groups of 10 mice each. Group 1 and 2 were treated before (preventive approach and group 3 and 4 after (therapeutic approach) development of proteinuria ≥100mg/dl. Two additional groups included 20 MRL/lpr mice which were prophylactically injected with SERPINB3 (10 mice, group 5) or PBS (10 mice, group 6).

The second experiment involved 30 NZB/W F1 mice which underwent subcutaneous immunization with PTX3+alum (n=10), PBS+alum (n=10) or PBS alone (n=10) three times three weeks apart, starting before development of proteinuria. For both experiments, time of occurrence and levels of anti-dsDNA and anti-C1q antibodies, proteinuria and serum creatinine, overall- and proteinuria-free survival were assessed in mice followed up to natural death. Subanalysis regarding anti-PTX3 antibody levels and function were performed in the second experiment.

The last experiment on mice involved 22 NZB/W F1 female littermates divided into two groups of 10 mice each and treated with the same approach described in the second experiment. Ten mice

(5 from each group) were sacrificed at week 22 and the other 10 at 29 weeks. Histological and ultrastructural lesions were compared using optical microscopy, immunoelectron microscopy (IEM), immunofluorescence (IF) and confocal microscopy.

Data on humans were retrieved enrolling 38 SLE patients (12 with biopsy-proven LN and 26 without LN) and 22 matched healthy donors (HD). Characterization and comparison of circulating levels of PTX3 specific (PTX3+) B cells between patients and controls was performed by flow-cytometry.

The differences between groups for nonparametric continuous variables were analyzed using Mann-Whitney U test or Kruskal-Wallis's ANOVA test when appropriate; proteinuria-free survival rate (proteinuria <300 mg/dl) and survival rates were evaluated by Kaplan-Meyer method using Mantel-Cox test for comparison. Chi-squared test was used for histological comparison. A p value<0.05 was considered statistically significant.

Results. Experiments on mice showed positive results in terms of clinical effects deriving from restoration of SERPINB3 levels or immunization with PTX3. SERPINB3-administered mice displayed a milder LN, with lower and delayed occurrence of nephritogenic antibodies and milder proteinuria at several timepoints, as well as a prolonged survival versus PBS groups. Immunization with PTX3 evoked a vaccine-like response with occurrence of anti-PTX3 antibodies only in immunized mice and delayed and decreased levels of nephritogenic antibodies and proteinuria, resulting in a significantly longer disease-free and overall survival.

Among mice sacrificed at given timepoints, notable differences were observed at IEM, IIF and confocal microscopy. PTX3-immunized mice displayed less or no electron-dense deposits (EDD) along the glomerular basement membrane and the mesangium, and remarkably decreased glomerular deposition of IgG, C1q and PTX3 compared to PBS-treated mice. Moreover, PTX3 was found inside the EDD at IEM and was shown to co-localized with nuclear material.

LN patients displayed significantly lower levels of circulating PTX3+ B cells in comparison to SLE and HD, showing a persistent decrease among naïve and memory PTX3+ specific subsets.

Conclusions. Clinical improvement of a lupus-like disease following restoration of SERPINB3 levels and immunization with PTX3 in lupus murine models suggests that very early abnormalities affecting molecules involved in tissue homeostasis, apoptosis and removal of apoptotic debris may induce further development of SLE and SLE-specific manifestations within an unpredictable lag time. PTX3 more strikingly emerged as a novel antigen in LN progression and PTX3/anti-PTX3 immunity appear to function as an early level of regulation which may fail in patients developing LN. Consistently, acquisition of a targeted anti-PTX3 immunity could hinder the progression from the preclinical to the clinical stages of disease. Altogether, these findings may add a piece of knowledge on the mechanisms supporting LN development and progression, and suggest that a targeted modulation of the native immunity could improve renal manifestations in selected patients. In the short term, dosage of serum anti-PTX3 antibodies may become a handful tool to help in stratifying lupus patients according to the risk of developing LN.

INTRODUCTION

Clinical and histological considerations

Lupus glomerulonephritis (LN) is one the most severe and common manifestations of SLE, affecting up to 50% of patients during their disease course and leading to considerable morbidity and mortality if not properly treated (1, 2). In fact, the rate of renal response following initial treatment is low and the proportion of patients maintaining a long-lasting response is lower than 50% (3), with a remarkable 40% of patients still developing some degree of renal impairment in the long term (4), culminating in ends stage renal disease in 10% of the cases (5). These still unsatisfactory results may reflect the incomplete understanding of the underlying pathogenic mechanisms driving LN development as well as a gap of knowledge between lesions that can be classified and their comprehensive clinical expression.

In fact, the current LN classification is mostly based on the elementary histological lesions affecting the lupus glomeruli, which raised some criticism and need for empowerment, as the histological picture itself is more complex than it is currently categorized demanding for instance a greater thoughtfulness of tubule-interstitial lesions and of factors that mostly impact patient prognosis (6,7).

Elementary histological lesions in LN include proliferative active lesions, i.e. endocapillary hypercellularity with narrowing of capillary lumen, karyorrhexis, fibrinoid necrosis and eventual rupture of the glomerular basement membrane (GBM), cellular or fibrocellular crescents due to extracapillary proliferation of resident and inflammatory cells, subendothelial deposits, endoluminal aggregates of immunecomplexes (IC) named *hyaline thrombi*, together with chronic lesions, i.e. glomeurlosclerosis, adhesions and fibrous crescents (8,9). Hence, the GBM is considered the initial target of glomerular injury, paving the way to widespread alterations affecting the whole glomerular tuft, the mesangium and the tubule-interstitial compartment. The

underlying pathogenic mechanisms have been not fully clarified so far in humans, with most information being retrieved from lupus mouse models (10-12).

Immune mechanisms of damage

Likely mechanism responsible for glomerular inflammation and damage include both immune and non-autoimmune drivers. Among the formers, a relevant role is attributed to nephritogenic antibodies, among which anti-chromatin/anti double stranded (ds) DNA and anti-C1q are the best characterized (13-16), which would initiate and sustain a type III reaction through the activation of the classical complement cascade. In fact, IC localized in the subendothelial space may directly harm endothelial cells and access the vascular space where they can activate the complement and trigger recruitment of inflammatory cells; conversely, IC deposition in the subepithelium is associated with prominent podocyte damage with relatively milder inflammation (8,9).

Beside, release of pro-inflammatory mediators and infiltration by immune cells are also relevant. In fact, IC can activate resident and immune-competent infiltrating cells to release pro-inflammatory cytokines such as CCL2 (CC-chemokine ligand 2) and TNF (tumor necrosis factor), which are likely to sustain the local inflammation (8) and accumulate progressively along with LN progression (17).

Among immune cells infiltrating the inflamed glomeruli, macrophages and neutrophils are key players. They sustain inflammation and enrichment of the autoantigenic pool by releasing pro-inflammatory cytokines, metalloproteases and NETs (neutrophil extracellular traps), which trap chromatin and nuclear antigens rendering them accessible to autoantibodies, while on the other hand blood-derived macrophages can contribute to aberrant fibrosis as a consequence of a switching toward a reparatory phenotype in response to the long-standing local inflammation (18,19). These mechanisms are likely to be entangled and may not have the same relevance among

different patients or even across different units in the same kidney. Consistently, variable gene signatures have been identified in renal samples of LN patients, suggesting that a predominant expression of neutrophil-related over lymphocyte-related genes as well as an increased expression of interferon (IFN)-related genes could predict LN development and a more aggressive LN course (20,21), thus highlighting the discrepancy between a molecular classification and the current histological ones.

Non immune mechanisms of damage

Non immune mechanisms develop concomitantly with the immune response, yet they are difficult to target due to their smoldering nature. They include a progressive fibrosis mostly sustained by mounting alterations in the endothelial structure and disrupted interactions with neighbor cells such as podocytes and mesangial cells, finally resulting in an unbalance between pro- and anti-inflammatory cytokines toward an uncontrolled release of fibrotic mediators including TGF (Transforming Growth Factor)-β and PDGF (platelet-derived growth factor), which lead to mesangial hyperproliferation and release of extracellular matrix (8). Moreover, interstitial pericytes lose their contact with tubular capillaries and migrate into the interstitial space where they can turn into myofibroblasts, thus enriching to pool of cells capable of secreting pro-fibrotic mediators beside macrophages, mesangial cells and podocytes (8). Unbalanced fibrosis leads to anatomical distortion of several renal districts consequently affecting the blood supply; chronic hypoxia is further worsened by a diminished expression of VEGF (Vascular Endothelial Growth Factor)-A and FGF (Fibroblast Growth Factor)-2 by endothelial cells, overall leading to a decreased perfusion of both glomeruli and tubuli (22). As loss of nephrons cannot be compensated due to their limited regenerative capacity, residual units undergo a functional overload with increased internal pressure, causing glomerular deterioration and further vascular deprivation also affecting the interstitium, as it usually receives blood from post-glomerular vessels that are

compromised by glomerular hypertension and fibrosis (8). The overall architecture is then completely altered, eventually leading to renal failure.

All the mentioned mechanisms play a synergic role in the establishment of renal damage. As the focus of our work resides within the immune mechanisms and especially in understating the role of PTX3-anti-PTX3 related immunity, in the next sections we will selectively deepen some of the mechanisms and players involved in those pathways.

The role of antibodies in LN

Anti-dsDNA antibodies

Anti-dsDNA antibodies are a well characterized marker of SLE with a well-known correlation with renal involvement (13,23,24). However, despite they have been used for a long time both as a follow-up tool and predictors of LN flares (14,23), their target antigens and their origin have not been clear-cut defined.

Anti-dsDNA antibody generation

The presence of isotype switched, somatically mutated anti-dsDNA immunoglobulins (Ig)G implies the occurrence of a T-dependent B cell autoimmune response against nucleic acids, which are not naturally immunogenic. Two major hypotheses have addressed this issue since a long time, yet not leading to a conclusive picture. The first is the hapten-carrier hypothesis (25,26) by which non-immunogenic DNA bound to a T-specific peptide would be able to evoke a T-helped B response. Indeed, because T helper cells cannot be activated in a cognate fashion by DNA alone, autoreactive B cells in lymph nodes would internalize circulating DNA bound either to exogenous peptides e.g. bacterial or viral proteins (27) or to endogenous peptides, e.g. histone-derived peptides binding DNA in the form of nucleosomes (28). B cells would then be able to process the

DNA-peptide complex and to present the sole peptide loaded onto Major Histocompatibility Complex (MHC) II molecules to autoreactive dormant T cells in secondary lymphoid organs (29). Hence, T cells would be primed to recognize the carrier (peptide) that had rendered its hapten (DNA) immunogenic. Activated T cells would then help B cells bearing a DNA-dedicated B cell receptor (BCR) to expand and mature into antibody secreting cells (30).

In this view, both foreign- reactive (e.g. virus-dedicated) and autoreactive T cells would be able to trigger an autoimmune response leading to production of nephritogenic antibodies. This hypothesis was experimentally demonstrated by immunizing mice with dsDNA chromatin fragments in complex with a peptide from T. cruzi (31) or with a complex of polyomavirus T antigen and chromatin fragments (28) with successful induction of anti-dsDNA antibodies.

One may argue whether histone-specific autoreactive T cells are the sole endogenous T cells responsible for anti-dsDNA antibody production (30). According to the second hypothesis i.e. the autologous-hapten hypothesis on anti-dsDNA generation, B cells are able to present fragments of their own BCR on MHC II molecules, namely endogenous Ig variable-region determinants (IgV), to idiotypic-specific T cells which may in turn help a secondary B-cell response (32). Experimental data in mice have shown that B cells may internalize fragments of complementary determining region (CDR)3 (33) or process newly synthesized intracellular Ig and present them to specific T cells in an immunogenic fashion (34)eventually leading to germinal center (GC) formation and isotype switching (32), provided BCR ligation occurs (35).

Idiotypes can be presented by either B cells or other antigen presenting cells (APC) through receptor-mediated endocytosis. Evidence of this process was obtained *in vitro* (34) and remade in both lupus models (32) and nonautoimmune mice (36) which developed lethal autoimmune-driven organ failure when rendered transgenic for Ig L chain and T cell receptor (TCR) (37).

Interestingly, anti-idiotypic specific T cells appear at a growing rate in sera of mice double-transgenic for a Ig L chain and an idiotype-specific TCR as they get older (37), which may be due

to the increased rate of BCR maturation and somatic hypermutation resulting in novel idiotypic peptides that are recognized by idiotypic specific T cells escaped from central tolerance. The fact that such self-antigen presentation may lead to an undisturbed secondary response may be explained by at least three concurring circumstances; i) tolerizing pressure leading to deletion of idiotypic-positive T cells is limited due to the hidden and above all casual nature of the B IgV formation in the bone marrow; ii) activated B cells and/or professional APC present somatically mutated V-region determinants (34) that are broadly unknown to the immune system; iii) heavy chain CDR3 idiotypes of anti-dsDNA antibodies show similarities with both histone-derived and microbial peptides that can trigger cross-reactivity of T cells (38). Limitation to the in vivo relevance of this mechanism mainly reside in that the amount of idiotypic-specific T cell clones and the chance of self T-B collaboration are low under physiological conditions, nevertheless it should be considered as a potential empowering trigger to autoantibody production.

Antigen recognition by anti-dsDNA antibodies

The issue on what antigens anti-dsDNA antibodies really bind is still open, and the dichotomy between direct binding and crossreactive antigen recognition is not completely solved (14).

Antibodies binding DNA

The big family of anti-dsDNA includes antibodies directed toward either relaxed DNA, i.e. the linker DNA connecting nucleosomes with each other, or bent DNA, i.e. packed nucleic acids inside the nucleosome structure (39). Moreover, they may recognize single-stranded(ss)DNA within dsDNA or Z-DNA, i.e. the left-handed amount of DNA present within the cells (40). Anti-dsDNA antibodies are capable of recognizing B-DNA, which is the widespread right-handed double helix loop populating cell nuclei. However, recognition of sole nuclear antigens is unlikely to trigger a durable autoimmune response, while nucleosomes and DNA are rendered more immunogenic by presentation on microparticles released from dying cells (41), which form IC and are subjected to

IgG binding (42). Levels of microparticles covered with IgG in sera of SLE patients were seen to correlate with levels of anti-dsDNA antibodies, being also associated with presence of anti-histone and even anti-extractable nuclear antigen antibodies (40,42). Moreover, microparticles can load IgM and IgG thereby enhancing complement activation and may undergo post-apoptotic modifications such as citrullination, glycosylation, and partial proteolysis which trigger the generation of neoantigens (42).

Antibodies binding nucleosomes

Nucleosomes are the fundamental subunit of chromatin and consist of approximately 146 DNA base pairs wrapping around a histone octamer made up of two copies each of histones H2A, H2B, H3 and H4, which are stabilized by the linker histone H1 binding across the nucleosome surface (43).

The peculiarity of nucleosomes in SLE resides in that they work both as driving antigens and as renal target for LN development (44) as abnormally exposed chromatin fragments derived from apoptotic cells can undergo post-apoptotic modifications until secondary necrosis and may represent a trigger for generation of anti-nucleosome antibodies (45). Early intraglomerular apoptosis was indeed demonstrated in LN murine models (46) and nucleosome-anti-nucleosome colocalization in electron-dense deposits (EDD) was shown in early phases of murine (47) and human(44) LN, suggesting nucleosomes may be released by dying cells and become immunogenic in the extracellular space, thereafter mediating the binding of nucleosome-complexed autoantibodies to the GBM.

Anti-nucleosome antibodies have shown even greater sensitivity versus anti-dsDNA antibodies in predicting active SLE, being detectable in sera of lupus patients before development of overt disease (48) and showed a direct correlation with disease activity and anti-dsDNA antibody levels (49).

However, the real prognostic value of anti-nucleosome autoantibodies in disease monitoring was challenged due to lack of agreement among laboratory assays used to detect anti-nucleosome antibodies following the absence of a unified definition of anti-nucleosome antibody specificity, which can lead to false positive results (50).

Autoantibodies cross-reacting with glomerular antigens

A great deal of cross-reactivities has been attributed to anti-dsDNA antibodies either in or outside the GBM, which could be proven in vitro (51,52), leading to the hypothesis they may directly bind crossreactive autoantigens within the kidneys and as such initiate the inflammatory process in LN (53). The putative mechanisms by which anti-dsDNA antibodies could recognize non-nucleosomal antigens are based on sharing of common tridimensional structures (51), molecular mimicry (52) or charge-charge interactions (51).

Glomerular antigens that were mostly proposed as native targets of anti-nucleosomes antibodies include alpha-actinin (α-actinin), alpha-enolase (α-enolase), type IV collagen, laminin, cardiolipin, heparan sulfate (HS), Annexin (51,52).

High levels of anti- α actinin antibodies were found in sera and kidney elutes of lupus prone mice (54) and immunization of non-autoimmune mice with α-actinin resulted in antinuclear antibody production and proteinuria (55). Unfortunately, no stable binding was further demonstrated in vivo of anti-dsDNA to α-actinin (56,57) and no relationship was established between serum anti-α-actinin antibodies and renal disease (57), with prospective studies on serum biomarkers having discarded anti-αactinin in respect of anti-C1q or anti-chromatin antibodies as a reliable LN biomarker (58).

Annexin A2 is a calcium dependent, phospholipid binding protein that can translocate from the cytoplasm to cell surface once the cell is activated (59) and was also proposed as a cross-reactive autoantigen of anti-dsDNA antibodies (60). Anti-dsDNA antibodies from LN patients have been shown to bind annexin A2 on mesangial cell surface and activation of proinflammatory molecules

following antibody internalization has been postulated (61); however, the exact mechanism, if any, accounting for anti-annexin A2 pathogenicity is still unknown (62).

Little evidence is available concerning the role of anti-laminin antibodies. The most abundant glomerular isoform of laminin is laminin-1 which is usually limited to the mesangial matrix and GBM but can be found in subepithelial deposits in inflamed kidneys (63). Passive transfer of anti-laminin-1 antibodies cross-reacting with anti-dsDNA antibodies in MRL/lpr mice led to formation subepithelial immune deposits and proteinuria (64), but on the other hand no specificity for laminin was found among antibodies eluted from nephritic lupus kidneys, while specificity toward nucleosomes and histones was proven (57). Interestingly however, laminin could play a role in bridging nucleosomes-anti-chromatin complexes to the GBM due to its negative charges, as suggested by a relatively high affinity of nucleosomes for laminin in vitro (Kd 10-9 M) (50); however, firm data in vivo are still lacking.

Finally, data supporting the aforementioned mechanisms of homology of tridimensional structures, molecular mimicry or charge interactions for anti-dsDNA cross-reactivity are scarce, as no common structural motifs or biochemical characteristics were really identified among most of the suggested cross-reactive antigens (51), and reactivity of SLE serum toward those molecules could have been misled by non-specific binding of nucleosome-associated proteins to residues on the putative cross-reactive antigen, thus resulting in a falsely enhanced reactivity (65). Moreover, even if cross-reactivity would be real at the beginning, the progressive affinity maturation of anti-dsDNA antibodies would likely select mutations recognizing dsDNA i.e. the BCR-specific antigen rather than crossreactive antigens, suggesting that any cross-reactive specificity would wane over time (14).

Taken together, evidence is conflicting around the true pathogenic role of cross-reactive antibodies *in vivo*. The major concern around non-nucleosomal antigens resides in that in vivo-bound antibodies have only been detected by electronic microscopy in EDD localized in the GBM and in

mesangial matrix, which have been previously pinpointed as the founding foci of LN initiation (discussed below) whereas no antibodies were observed outside the EDD, suggesting that native GBM antigens are not targets of nephritic antibodies *in vivo* (46,57,66,67). Consistently, none of the molecules candidate to cross-react with antichromatin antibodies was ever found within the EDD (68) nor were seen to correlate with renal pathology (57), suggesting that they may arise as an epiphenomenon rather than entailing a real pathogenic role.

Antibodies that amplify renal inflammation

Once LN is established, the inflammatory loop in the kidney is maintained by antibodies able to perpetuate inflammation. Among them, the best characterized are C1q antibodies, whereas evidence is conflicting on other autoantibody targets.

Anti-C1q

Anti-C1q antibodies are found in 40% to 60% of lupus patients, yet they are present in other autoimmune diseases (69) as well as in healthy individuals (70). They are not specific to SLE, however their contribution to LN and renal flares has been suggested since a long time (71,72). They have been shown to follow variation of disease activity and to decrease after successful treatment (73), performing even better than antidsDNA antibodies as serological biomarkers (74).

Despite growing evidence supporting a role for anti-C1q antibodies in LN progression, the precise mechanism is still elusive. Current knowledge supports a role for anti-C1q antibodies in increasing complement activation, as they could favor IgG clusterization on apoptotic cells and thereby facilitating complement fixation, *via* both the classical and the lectin complement pathway (16). Consistently, complement activation was analyzed by measuring deposition of terminal complement fragments on section of lupus kidneys and was found to be increased in presence of anti-C1q antibodies (16).

It could be speculated that like anti-dsDNA and anti-chromatin antibodies anti-C1q become pathogenic only in presence of abnormal autoantigen availability and/ or anti-C1q-containing IC in the kidney (75), as under those conditions anti-C1q antibodies may trigger inflammation via either complement activation or Fc engagement on immune cells. This would lead in turn to a decreased availability of C1q due to consumption, persistence of apoptotic remnants, increased complement fixation and consecutive renal injury in a self-maintaining vicious cycle.

Antibodies against podocyte antigens

Overall, it was estimated that anti-DNA antibody deposition accounts for about 10-20% of eluted IgG from nephritic kidneys (76). Although this proportion may be sufficient to incite renal damage, the vast majority of glomerular target antigens beside chromatin antigens remains unknown. Observations have shown podocyte damage to occur in LN (77) and suggested urinary excretion of podocyte-associated mRNA to correlate with proteinuria, reflecting a worse glomerular damage (78). An Italian research group carried out an elegant study in which they dissected glomeruli from sample biopsies of SLE patients affected with LN, demonstrating that glomerular IgG recognize a panel of 11 podocyte antigens, with antibodies against α-enolase and Annexin A1 predominating over others (79,80). It is worth noting that podocyte antigens did not cross-react with dsDNA and purified anti-dsDNA antibodies did not recognize α-enolase, thereby excluding a cross-reactivity with chromatin antigens (79).

Currently, the pathogenicity of anti-podocyte antibodies has hardly been tested in vivo. Intraperitoneal injection of hybridomas secreting anti-αenolase antibodies in BALB/c mice resulted in mild proteinuria in 25% of mice, suggesting they have a limited nephrotoxic potential (79), despite previous experiments investigating the evolution of the antibody response in NZB/W F1 mice showed an ordered occurrence of autoantibodies in male littermates, with anti-α-enolase appearing quite late in time (81). However, those observations were not confirmed in female

NZB/WF1 mice and should be interpreted in the light of a strong genetic background influencing the antibody response.

Proposed unifying models for development of LN: state of the art

As discussed above, historically two mutually exclusive theories attempted to explain the attachment of anti-chromatin antibodies to the GBM and the subsequent initiation of inflammation. The first hypothesis (the cross-reaction model) states that anti-chromatin antibodies could cross-react with glomerular antigens such as αactinin or collagen, thus suggesting that LN would be driven by a polyclonal B cell activation, which in turn would allow the activation of the complement cascade. Conversely, the second hypothesis (the chromatin model) suggests that anti-chromatin antibodies can bind to the GBM *via* nucleosomes, thus targeting abnormally exposed nuclear antigens which would confer the antibodies themselves a true pathogenic value (14).As aforementioned, growing evidence seems to be more in support of the second hypothesis, as despite *in vitro* cross-reactivity of anti-chromatin antibodies toward a wide array of antigens, the same could not be convincingly proven *in vivo* (discussed above).

Assuming binding to nucleosomes as a more likely mechanism for anti-chromatin antibodies to attach to the GBM and result in renal inflammation, two main hypothesis aim at explaining the nature of this binding, which could be either direct (antigen-planted) or indirect, i.e. mediated by negatively charged glycosamminoglycans able to bridge the antibody-nucleosome IC to the GBM (planted immunecomplex theory) (44,46). So far, more data seem to support the latter view, as purified anti-dsDNA antibodies do not bind the GBM directly, while anti-chromatin-nucleosome IC do (82), thus suggesting nucleosomes would mediate the link. In fact, experimental evidence has shown that intrarenal perfusion of nucleosome-autoantibody complexes could lead to intense glomerular binding, while perfusion with sole purified nucleosome-free anti-chromatin antibodies could not (82). The underlying suggested mechanism is that the binding of anti-chromatin

antibodies to the nucleosomes could mask nucleosome r inherent negative charges, allowing connected histones, which are positively charged, to bind to negatively charged residues on the GBM, e.g. HS or collagen IV, thereby indirectly anchoring the anti-chromatin-nucleosomes IC to the GBM (51). Consistently, masking of positive histone charges by addition of heparin, which is structurally similar to HS, as well as treatment of the GBM with collagenase IV prevented the deposition of IC in the GBM and further development of proteinuria (47, 83).

The gap of the events occurring from autoantibody deposition to renal inflammation was not filled so far, although a unifying model for LN development was proposed based on observations in murine models of SLE (15). The hypothesis highlights a two-step mechanism sustained by abnormal accumulation of nuclear material in the extracellular matrix, overwhelming of scavenging mechanisms and autoantibody deposition with initiation and propagation of inflammation. The first step is supposed to reside in abnormalities affecting the apopotic process in the lupus kidney which would lead to an increased exposition of non removed cellular and nuclear antigens further acquiring immunogenicity following post-apoptotic modifications (44). Circulating anti-chromatin antibodies would then be able to bind nucleosomes and locally form IC, which would further saturate the scavenging potential of mesangial cells, leading to secretion of additional mesangial matrix serving as a platform for further accumulation of ICs, thus establishing a silent mesangial nephritis (15). It should be mentioned that aberrant accumulation of nuclear material was supposed to itself ignite the generation of anti-dsDNA antibodies; although likely, this mechanism was not demonstrated so far, notwithstanding nuclear antigens being the main targets of anti-chromatin antibodies in vivo (14,44).

The second step is the transition from a mesangial nephritis to a proliferative glomerulonephritis which would be promoted by the loss of expression of DNAse I . DNAse I is the most important endonuclease in the kidney, where it cuts chromatin fragments helping their removal (14). Reasons for selective down-regulation of DNAseI expression in the lupus kidney are not known although

its occurrence was shown both in lupus models of LN (84,85) and human SLE (86). Hence, the abrupt loss of its endonuclease function joint with a persistent activity of metalloproteinases in the lupus kidney (85) would increase the deposition of abnormally big chromatin fragments enriched with a great burden of epitopes even beyond the mesangium, thus providing room for IC deposition outside the mesangial matrix to the GBM, thus initiating a self-maintaining loop eventually culminating in massive complement fixation and inflammation.

Role of SERPINB3, PTX3 and anti-PTX3 antibodies

The picture of LN development entails so far several open pathways to be characterized. In our research field, we investigated the role of some molecules which are likely to undergo disturbances along SLE development and may be involved in LN initiation and progression.

SERPINB3

The rationale for exploring the function of SERPINB3, an actual cystein protease inhibitor belonging to the SERPINS (Serin Protease Inhibitors) superfamily, in SLE was driven by two points: first, SERPINB3 is involved in a number of functions related to tissue homeostasis, including protection from infections, pregnancy and most importantly cell survival (87,88), and second SERPINB3 expression is reduced on SLE CD27+ B cells as well as on CD27+ cells of patients with hepatitis C (HCV) infection, leading to the discovery that IFNα mediates SERPINB3 gene repression (89), thereby suggesting that patients with a prominent IFNα signature may be subjected to a deep loss of SERPINB3.

SERPINB3 is an ancient molecule, evolutionary conserved from simple organisms to mammals, suggesting that it plays a fundamental role in physiological functions and that its alterations may foster abnormalities in several domains of tissue homeostasis, including the immune system. In fact, evidence has highlighted an increased expression of SERPINB3 across several types of solid

cancers, including cervix carcinoma, esophagus carcinoma, head and neck carcinomas, as well as liver cancer (90,91), where its expression correlated with increased tumor invasiveness and poor prognosis. These findings were at least in part attributed to an increased resistance to cell death as SERPINB3 was also shown to influence the intrinsic and extrinsic apoptotic pathways (88) resulting in overall resistance to apoptosis. Underlying mechanisms are thought to be inhibition of caspase 3 or upstream proteases, preventing cytochrome c release from mitochondria in response to oxidative stress conditions (90) as well as inhibition of reactive oxygen species (ROS) generation through binding of respiratory Complex I in the inner mitochondrial compartments, leading to hindrance of the opening of the permeability transition pore, a point of no return in cell commitment to death (92). In addition, decreased phosphorylation of the proapoptotic molecule p38 MAPK (mitogen-activated protein kinase) or of the active forms MKK3/6 was shown in engineered 293T cells overexpressing SERPINB3, thus suggesting an additional mechanism of apoptosis inhibition (93). Thus, decreased SERPINB3 expression in SLE may result in increased apoptotic rate, likely increasing the antigenic burden and contributing to aberrant immune responses in SLE.

We therefore investigated the effects of SERPINB3 restoration in a mouse model of lupus in terms of survival and development of nephritogenic antibodies and a lupus-like nephritis (**Paper I,** discussed below).

PTX3/anti-PTX3 immunity

Pentraxin 3 (PTX3) is an octameric glycoprotein belonging to the long pentraxin family i.e. multimeric evolutionary conserved molecules acting as acute-phase reactants, being mainly locally released at sites of inflammation by either immunocompetent or resident cells (94). PTX3 can be released by neutrophils, monocytes, lymphocytes, epithelial as well as mesangial cells following exposure to proinflammatory stimuli such as TNFα or IL-1, being not affected by IL-6, unlike

short-chained pentraxins (95). PTX3 shares a 200-aa long common pentraxin C-terminus with short pentraxins yet entailing a peculiar N-terminus with no homology to other proteins possibly involved in PTX3 functions ranging from anti-microbial first line defense to tissue homeostasis, through modulation of the immune response (94). PTX3 can bind a wide array of microbes *via* recognition of microbial moieties further functioning as an opsonin or increasing the macrophage phagocytic potential (95).-Additionally, PTX3 it is able to offer binding sites for diverse molecules such as C1q or Fibroblast Growth Factor-2 and for the extracellular matrix including the oophorus cumulus (97,98), and to establish a binding with either living cell types, such as dendritic cells, or apoptotic cells (99,100). The binding of PTX3 to marginal zone (MZ) B cells was described which promoted production of IgM and IgG antibodies by these B cells, thus suggesting a novel B helper function of PTX3 (101). So far, the binding site of PTX3 other than Fcɣ receptors or Toll-like receptors (101) was not precisely characterized.

Moreover, PTX3 is extensively involved in ischemia/reperfusion injury (recently reviewed in (102)) and regarding the kidney it was shown to locally accumulate following tissue injury, where it can hinder excessive damage by decreasing P-selectin expression on endothelial cells and subsequent leukocyte recruitment.

Interestingly, PTX3 effects are multifaced and influenced by the surrounding environment. Importantly, the multifaceted interaction of PTX3 with the complement system is being unraveled by previous and recent evidence (103). Under physiological conditions, PTX3 bound to foreign antigens is able to initially activate the complement pathway through its antibody-like functions upon recognition of repetitive moieties on pathogens (96,104), yet subsequently giving rise to a feedback loop which prevents excessive complement activation by recruiting inhibitory factors such as factor H and C4 binding protein (C4BP) (103).

The interaction with the classical complement pathway is complex and influenced by the availability of apoptotic debris to which PTX3 can bind. Indeed, *in vitro* studies have shown that

the soluble isoform of PTX3 binds and sequesters C1q through binding to its globular heads thereby preventing complement activation, while PTX3 bound to apoptotic debris is able to increase C1q deposition and further activation of the cascade (99,104,105), despite the binding sites of PTX3 and C1q on apoptotic cells are different. Actually, under physiological conditions, PTX3 binding to self remnants exerts a clearing effect preventing those remnants from being taken up and immunologically presented by APC (100). However, when the antigenic burden is overgrown, this homeostatic balance may be lost and turn PTX3 to function as a pure opsonin, thus shifting from an anti-inflammatory to a pro-inflammatory behavior (104).

In relation to LN, PTX3 may play a role connected to its local release by resident cells, to the capability of PTX3 to stimulate mesangial cells to secrete mesangial matrix (106,110), as well as to the aforementioned role in complement activation.

The interest of our group for PTX3 in LN was driven by the retrieval of anti-PTX3 antibodies in serum of SLE patients being inversely correlated with occurrence of LN in ours and other cohorts (108,109), suggesting they may exert protective effects against LN development. Moreover, deposition of PTX3 in human lupus kidneys correlated with the extent of fibrosis and proteinuria (110,111), suggesting that PTX3 may indeed contribute to damage in the lupus kidney. This led to the attempt of reproducing the same findings in a mouse model of lupus (**Paper II**, discussed below) *via* immunization of mice with human recombinant (hr)PTX3. Furthermore, we aimed at characterizing potential ultrastructural alterations induced by PTX3 immunization across target organs with a main focus on the kidney (**Paper IV, unpublished)**, discussed below). Beside, characterization of circulating PTX3-specific B cells in blood samples of SLE patients was also performed, exploring this novel autoantigen specificity in health and disease (**Paper III,** discussed below).

AIMS

The aim of the whole PhD project was to characterize possible novel immunomodulatory mechanisms in development of LN and especially to point out clinical effects and ultrastructural changes induced in the kidney by immunization with PTX3, whose role is under investigation as key antigen in LN regulation.

Specific aims were

- To investigate the effects on LN development and survival provided by the restoration of a pathologically down regulated molecule in murine models of LN, namely SERPINB3 (**Paper I**)
- To evoke a vaccine-like response to PTX3 in lupus-prone mice and to investigate the putative protective effects of anti-PTX3 antibodies on survival, serological changes and disease course of immunized versus control mice (**Paper II)**
- To identify circulating PTX3-specific B cells and to assess differences in distribution of PTX3-specific B cell subsets among SLE patients with or without LN compared to healthy controls (**Paper III**)
- To assess tissue changes induced following immunization with PTX3 and to provide insights on ultrastructural localization of PTX3 in respect to the glomerular structures and associated EDD in lupus-prone mice (Paper IV, unpublished).

METHODS

Paper I

Mice

In this experiment, 40 New Zealand Black/White (NZB/W F1, Harlan Laboratories, Envigo RMS, UD, Italy) and 20 MRL/lpr mice ((Harlan Laboratories)) were recruited and subdivided into different groups as described in the following sections. NZB/WF1 and MRL/lpr strains are well characterized models of SLE which spontaneously develop a lupus-like nephritis, starting from about 15-17 weeks of age, and a systemic lupus-like disease at 12-15 weeks, respectively (112). MRL/lpr mice additionally display a widespread lymphoadenopathy with a predominant double negative T infiltrate, erosive polyarthritis, severe necrotizing arteritis, neuropsychiatric symptoms and a severe proliferative nephritis leading to death between 3 and 7 months.

Treatment protocol

NZB/W F1 mice

Mice were treated with recombinant SERPINB3 either before (preventive approach) or after (therapeutic approach) the development of proteinuria.

Preventive approach

Twenty 12-week-old NZB/NZW F1 female mice were subdivided into 2 groups of 10 mice each and intraperitoneally injected with a total volume of 100 μl consisting of 7.5 μg of SERPINB3 in 100 μl of phosphate buffered saline (PBS, vehicle) (group 1) or 100 μl of vehicle (group 2). Mice were injected twice a week, starting from the 17th week of age, and bred until natural death, except three mice from both groups which were sacrificed at week 27. Kidneys of mice sacrificed at week 27 (3 belonging to group 1 and 3 to group 2) were harvested for histological comparison.

Therapeutic approach

Twenty 12-week-old NZB/NZWF1 female mice were subdivided into 2 groups of 10 mice each and were intraperitoneally injected with a total volume of 100 μl consisting of 15 μg of SERPINB3 in 100 μl of vehicle (group 3) or 100 μl of vehicle alone (group 4). Mice were injected twice a week, starting after development of proteinuria ≥100 mg/dl, and bred until natural death. Kidneys from 6 mice were harvested at death for histological examination, but were not included in the comparative analysis.

MRL/lpr

MRL/*lpr* mice were treated with recombinant SERPINB3 before the development of proteinuria in order to explore the preventive approach in a multiorgan system.

Twenty 8-week-old MRL/lpr female mice were subdivided into 2 groups of 10 mice each and were intraperitoneally injected with a total volume of 100 μl consisting of 7.5 μg of SERPINB3 in 100 μl of vehicle (group 5) or 100 μl of vehicle (group 6), as controls. Mice were injected twice a week, starting from the 9th until the sacrifice. Six mice were sacrificed at week 13 and 6 mice at 16–18 weeks. Time for sacrifice was chosen a priori, taking into account the age at which the disease is known to be full-blown (around 4 months). Kidneys were harvested from 12 mice at sacrifice for histological analyses.

Subdivision of mice into groups is depicted in **Table 1.**

Table 1. Mice group subdivision

	Preventive approach	Therapeutic approach
NZBW/F1		
SERPINB3	Group 1 n=10	Group 3 n=10
PBS	Group 2 n=10	Group 4 n=10
Mrl/lpr		
SERPINB3	Group 5 n=10	
PBS	Group 6 n=10	

NZBW/F1: New Zealand Black/White; PBS: phosphate buffer saline

Measurement of autoantibodies

Levels and time of occurrence of anti-dsDNA and anti-C1q antibodies were evaluated by by indirect ELISA assays performing a systematic blood collection from the caudal vein at the 17th, 21st, 25th, 28th, 32rd week of age, and at death. ELISA reagents were purchased from Sigma, St Louis, USA; ELISA plates were purchased by Nalgene Nunc, New York, USA.

For anti-dsDNA antibodies, plates were coated following 3 steps: addition of poly-L-lysin at a concentration of 10 μg/ml, in order to catch the DNA; then addition of calf foetal dsDNA at a concentration of 25 μg/ml; finally, addition of poly-L-glutamate at a concentration of 5 μg/ml in order to neutralize the free negative charges of DNA. Plasma were added in duplicate diluted 1:100 in 1% BSA/PBS. Alkaline phosphatase-conjugated goat anti-mouse IgG was added at the concentration of 100 ng/ml in 1% BSA/PBS. Finally, p-nitrophenyl phosphate was added. The plates were read at 405 nm.

For anti-C1q antibodies, plates were coated with C1q at a concentration of 5 μg/ml. Plasma were added in duplicate diluted 1:4 in 1% BSA/PBS with 1M NaCl, to prevent immune complex formation. Alkaline phosphatase-conjugated goat anti-mouse IgG diluted 1:10000 in 1% BSA/PBS with 1M NaCl was added. Finally, p-nitrophenyl phosphate was added. The plates were read at 405 nm.

Evaluation of proteinuria

Disease progression was monitored by weekly urine sampling in order to evaluate proteinuria levels, using multireactive strips (Siemens) and expressed as mg/dl. Proteinuria was evaluated according to the manufacturer: negative, slight positive, positive: + = 30 mg/dl, ++ = 100 mg/dl, +++ = 300 mg/dl and ++++ ≥2000 albumin. Traces of proteinuria were defined as 15 mg/dl.

Flow-cytometry

The basis of flow-cytometry is to analyze cells flowing in single files in front of a laser, so that they can be detected, counted and sorted. Cell components are labelled with a fluorofore that emits light once hit by the laser ray at different wavelengths. The fluorescence can then be measured to determine the amount and type of cells within a sample.

In this experiment, ***s***ingle-cell suspensions were prepared from the collected splenocytes and incubated with APC-conjugated anti-mouse CD3, peridinin-chlorophyll proteins (PerCP Cy5.5)-conjugated anti-mouse CD4, phycoerythrin (PE)–conjugated anti-mouse CD25, FITC–conjugated anti-mouse FoxP3, PE- conjugated anti-mouse IL-17, or their respective isotype controls, for evaluation of T cell subsets. Staining for FoxP3 was conducted using an eBioscience FoxP3 staining kit. For detection of Th17 cells, T cells (1×10^6 cells/well) were incubated with 50 ng/ml phorbol myristate acetate and 1μg/ml ionomycin (Sigma) in the presence of brefeldinA 5μg/ml (Sigma) for 5 h, before intracellular staining. Samples were acquired using FACSCanto system (Becton Dickinson Immunocytometry Systems) and FlowJo software (Tree Star) was used for data analysis.

Histological analysis of the kidneys

Six NZB/WF1 mice sacrificed at week 27 underwent histological comparison (three from group 1 and three from group 2). Kidneys of 12 out of 20 Mrl/lpr mice were harvested for histological analysis and comparison; six out of 12 mice analyzed had been sacrificed at week 13 and 6 at

week 16–18.Renal sections as thin as 3 μm (microtome Leica RM 2145) underwent histopathological evaluation by optical microscopy, focusing on renal functional compartments (glomeruli, tubuli, interstitium, vessels).

In order to properly evaluate different renal compartments, specific histological stainings were used. Samples were fixed in formalin 10% and embedded in paraffine and then stained by Hematoxyline-Eosin (HE), Periodic Acid Schiff (PAS), Acid Fuchsin Orange G (AFOG), Masson Trichrome staining (TRIC) and Periodic Acid Schiff Methanamine (PASM).

Renal sections were then screened by experienced pathologists in a blinded fashion for presence of glomerular lesions (glomerulosclerosis and mesangial hyperplasia), perivascular inflammation and tubular lesions (tubular dilation and presence of casts), according to a semiquantitative score from 0-1 (no/mild involvement) to 4-5 (very high involvement) (112, **Table 2**).

Statistical analysis

The differences between groups were analyzed using Mann-Whitney U test for nonparametric continuous variables; proteinuria-free survival rate (proteinuria <300 mg/dl) and survival rates were evaluated by Kaplan-Meyer method using Mantel-Cox test for comparison. Analysis of covariance during time was calculated by ANOVA for repeated measures in MRL/*lpr* mice sacrificed at discrete time points. Within-group contrasts were performed according to Bonferroni's method. Results of ANOVA are presented reporting 3 F test values, namely F_G for grouping factor, F_T for time, and F_{GxT} for the interaction between time and grouping factors. Chi-squared test was used for histological comparison. Flow cytometry data were analyzed by Student's t test for independent samples. IBM SPSS Statistics 22 for Windows software (IBM SPSS Inc., USA) was used for calculations. A p value$\leq$0.05 was considered statistically significant.

Table 2. Semiquantitative scoring system to quantify renal lesions

	Score	Glomerular lesions		Tubular lesions		Interstitial lesions (perivascular inflammation)
		% of affected glomeruli	Severity of lesions	Tubular dilation	Casts (expressed as the number of affected nephrons)	
Mild	0	<2			0-1	Up to a few rare lymphocytes
	1	2-10	Segmental thickening of mesangium	Minimal dilation of few tubules, either as a focus or multifocal; generally limited to inner stripes of outer medulla	2-10	A few lymphocytes forming loose aggregates
	2	10-30	Segmental to diffuse thickening of the mesangium, most glomeruli	Minimal/mild dilation of up to 20% of the tubules either as a focus or multifocal; generally limited to inner stripes of outer medulla	11-20	Lymphocytes forming discrete small aggregates
Moderate	3	30-50	Diffuse thickening of mesangium, hypercellular glomerulus, increased size of podocytes, generally no adherences	Mild/moderate dilation of up to 50% of the tubules, expands to same areas of the cortex	20-30	Polarized aggregates of lymphocytes that bulge into the lumen of the adjacent vein but fail to fully surround the arcuate artery
Severe	4	50-70	Diffuse thickening of mesangium, my be coagulated proteins or fibrous, hypocellular glomerulus, increased size of podocytes and Bowman's capsule epithelium, adherences, crescents	Mild/moderate dilation of > 50% of the tubules, expands throughout the cortex	30-40	Lymphocyte aggregate fully surrounding the arcuate artery and not showing obvious polarization
	5	>70				Lymphocytic infiltrate extending from the adventitia of the arcuate artery into the adjacent connective tissue

Paper II

Thirty 8-week-old NZB/NZW F1 female mice were subdivided into 3 groups of 10 mice each and were subcutaneously injected with a total volume of 200 μl which consisted of 100 μg of hrPTX3 in 100 μl of PBS and 100 μl of alum in group 1, 100 μl of alum and 100 μl of PBS in group 2 and 200 μl of PBS in group 3. Mice were injected 3 times 3 weeks apart, before the development of proteinuria≥100mg/dl, starting from the 11th to the 17th week of age, and bred until natural death occurred.

Measurement of autoantibodies

Measurement of anti-dsDNA and anti-C1q autoantibodies was performed as described in Paper I, following blood collection before every injection (at the 11th,14th, and 17th week of age), at the 22nd, 28th, and 35th week of age, and at death.

In addition, levels and time of occurrence of anti-PTX3 antibodies were evaluated according to the following procedure: plates were coated with PTX3 at a concentration of 5μg/ml in PBS. Recombinant human PTX3 was obtained by purification from transfected Chinese hamster ovary (CHO) cells according to the protocol described by Bottazzi et al. (95). Plasma were added in duplicate diluted 1:100 in 1% bovine serum albumin (BSA) in PBS. After 4 hours incubation at room temperature and three washing steps, alkaline phosphatase-conjugated goat anti-mouse IgG 1:10000 1% BSA/PBS was added, and incubated for 1h at 37°C. After five washes, p-nitrophenyl phosphate was added. The plates were read at 405 nm.

Evaluation of proteinuria and serum creatinine

Disease progression was monitored by weekly urine sampling in order to evaluate proteinuria levels, using multireactive strips (Siemens) and expressed as mg/dl. Proteinuria was evaluated as

described in Paper I. Additionally, renal function was monitored through serum creatinine levels on blood samples withdrawn every three weeks starting from week 11 in mice from all groups. Creatinine measurement was carried out on Cobas 8000 (Roche Diagnostics) using an enzymatic method, traceable to Isotope Dilution Mass Spectrometry (IDMS) reference procedure.

In vitro assays on anti-PTX3 antibody function

To explore the putative anti-inflammatory properties of human anti-PTX3 antibodies, we investigated the type and the effects of anti-PTX3 antibodies on the *in vitro* interaction between C1q and solid-phase immobilized PTX3 through different ELISA assays.

In the first part of the experiment, ELISA tests to measure C1q binding to PTX3 in the presence or not of anti-PTX3 antibodies were set up. We tested sera from SLE patients positive (n=4) or negative (n=3) for anti-PTX3 antibodies, pooled serum samples from ten healthy subjects, and commercially available rabbit polyclonal IgG anti-PTX3, which were incubated at different dilutions with fixed concentrations of C1q on microtiters wells coated with hrPTX3 (5 ug/ml in PBS) and compared with PTX3 binding to the sole C1q (serially diluted C1q (Sigma) in PBS (from 0.020 to 10 mg/ml), in duplicate).

To determine the IgG4 subclass of human IgG anti-PTX3 antibodies, the already described anti-PTX3 assay (108) was modified to detect both total IgG and IgG4 anti-PTX3 antibodies, using as secondary antibodies either alkaline phosphatase-conjugated goat anti-human IgG (H þ L) antibodies, diluted 1:10000 in 1% BSA/PBS, or alkaline phosphatase-conjugated mouse monoclonal antihuman IgG4 antibodies (gamma chain-specific) (ab99816, Abcam), diluted 1:750 in 1% BSA/PBS. Background reactivity of ELISA reagents was checked in blank wells not incubated with serum samples, processed in parallel with tested wells. The cut-off value for IgG anti- PTX3 was derived from ROC curve analysis, as described previously (110), the one for IgG4 anti-PTX3 was determined as the mean plus 2 SD of the OD values obtained in 23 normal human

sera. IgG4 anti-PTX3 antibody positivity was expressed as both frequency of positivity (percentage values) and as percentage IgG4/IgG ratio (%) of the corresponding total IgG anti-PTX3 antibody amount, expressed as OD values.

Histological analysis of the kidneys

Kidneys were harvested from each mouse at death for histological analyses. Histopathological evaluations on kidney was performed by optical microscopy. Each biopsy was stained with H&E and PAS. Renal sections were screened in a blinded fashion for presence of glomerulosclerosis, mesangial hyperplasia and lymphocytic infiltrates. Semiquantitative score from 0 (no involvement) to 5 (very high involvement) was applied. Kidney sections further underwent immunoistochemistry using a commercially available rabbit polyclonal IgG anti-PTX3 (Alexis, Enzo Life Sciences, Lausen, Switzerland, 1 mg/ml). Immunostaining for detection of PTX3 glomerular deposits was performed on paraffin embedded kidney tissue, horseradish peroxidase (HRP)-conjugated anti-rabbit IgG as secondary antibody. Microwave and citrate as retrieval method at 1/1000 dilution was done. PTX3

staining was evaluated through a semiquantitative evaluation by selecting 5 high power field (HPF) (40x); for each field we evaluated 4 glomeruli (20 glomeruli in each kidney) and counted the positivity of PTX3 staining. PTX3 immunostaining was expressed as percentage of extension area of PTX3 positivity on the total area of glomeruli for each kidney. Complement deposition was also evaluated using a polyclonal rabbit anti-human C3d antibody (Dako, 0063, lot 017, 4.8 g/l). Microwave and citrate as retrieval method at 1/1500 dilution was done.

Statistical analysis

The differences among groups were analyzed using Kruskal-Wallis's ANOVA test; correlations were evaluated by Spearman's correlation test; proteinuria-free survival rate (proteinuria <300 mg/dl) and survival rates were evaluated by Kaplan-Meyer method using Mantel-Cox test for

comparison. Serum creatinine levels were expressed as median (min-max) and compared by Mann Whitney U test. Histological comparison was carried out using Mann Whitney U test for non parametric variables; comparison of PTX3 staining among groups was performed by ANOVA test corrected by Bonferroni. A p value < 0.05 was considered statistically significant. IBM SPSS Statistics 22 for Windows software (IBM SPSS Inc., USA) was used for calculations.

Paper III

Patients

Patients blood samples were analyzed in the study carried out in paper III, for which 38 consecutive SLE patients (American College of Rheumatology criteria (113)), including 12 with biopsy-proven LN, and 22 age-matched healthy controls were recruited at Charité Hospital (Berlin, DE) after signature of informed consent in accordance with the local ethics committee of the Charité Universitätsmedizin Berlin. Active LN was defined as proteinuria>0.5 g/day or creatinine clearance < 60 ml/min/1.73 m2, evaluated by Cockcroft and Gault formula, with active urinary sediment (114).

Flow-cytometry

To identify $PTX3^+$ B cells, purified hrPTX3 was labeled with either cyanine 5 (Cy5) or PE. PTX3 was labeled at the German Rheumatism Research Centre (DRFZ), Berlin. For flow cytometric analysis, the following fluorochromelabeled antibodies were used: PTX3 staining: anti-CD19 Allophycocyanin (APC)-Cy7 (clone SJ25C1, BioLegend), anti-CD20 Brilliant Violet (BV)510 (clone 2H7, BioLegend), anti-CD27 Fluorescein isothiocynate (FITC) (clone M-T271, BD), IgG PECy7 (clone G18-145, BD), IgD Peridinin-Chlorophyllprotein (PerCp) Cy5.5 (clone IA6-2, BD), anti-CD3/anti-CD14 Pacific Blue (PacB) (clone UCHT1/M5E2, BD).

PTX3+B cells were identified as B cells binding both PTX3-PE and PTX3-Cy5 After Fc receptor blocking (Miltenyi Biotec, Germany), stainings were performed in the dark at 4◦C for 15min, followed by two washing steps with PBS/BSA and centrifugation for 5min at 4°C and 330×g. Stained cells were analyzed by flow cytometry using a FACS Canto II flow cytometer (BD, USA).

B cell subsets were defined as naïve (single $CD3^{-}CD14^{-}Dapi^{-}CD19^{+}CD20^{+}CD27^{-}$), memory (single $CD3^{-}CD14^{-}Dapi^{-}CD19^{+}CD20^{+}CD27^{+}$) and plasmablasts (single $CD3^{-}CD14^{-}Dapi^{-}CD19^{+}CD27^{hi}CD20^{-}$).

Absolute numbers of B subpopulations were calculated by using the absolute number of B cells/µl retrieved with Multitest 6-color TBNK analysis (BD, USA) according to the manufacturer's protocol.

Statistical analysis

Samples included in analyses had at least 1×10^6 events with a minimum threshold for CD19+ cells of 50,000 events. Flow cytometric data was analyzed by FlowJo software 7.6.5 (TreeStar, Ashland, OR, USA). GraphPad Prism Version 5 (GraphPad software, San Diego, CA, USA) was used for statistical analysis. To test for significance, non-parametric tests were used. A p value <0.05 was considered statistically significant.

Paper IV (unpublished)

Mice

Twenty-two NZBWf1 female mice of 8 weeks of age were subdivided into two groups (group 1 and group 2) of 11 mice each.

Mice were subcutaneously injected following the prophylactic protocol described in Paper II, yet the alum+PBS group was not included as it was proven to be comparable to the PBS only group in terms of clinical and serological findings (Paper II). Group 1 mice were immunized with a total amount of 200 µl containing 100 µg of recombinant human PTX3 in 100 µl of PBS and 100 µl of alum (Sigma), while mice of group 2 were treated with a subcutaneous injection of 200 µl of PBS as control.

In order to evaluate disease progression at given timepoints *via* histological analysis of the kidneys, 5 mice from each group (10 mice totally) were scheduled to be sacrificed at the 22nd week of age while the other 12 mice (six from each group) at the 29th week of age.

Measurement of autoantibodies

Plasma levels of mouse anti-PTX3 antibodies were evaluated on blood collected at sacrifice, as described for Paper II.

Flow-cytometry

For flow cytometric analysis, blood samples were obtained from spleens and bone marrows. Half spleen was collected from each mouse and homogentated using a lanced. The homogenated spleens were filtered using filter with pore size of 70µm (BD Bioscience) and the eluted was collected into a 15mL falcon with 1mL of PBS. Bone marrows samples were obtained from femurs using a syringe to flush out the bone marrows from the bone. The bone marrows samples were similarly filtered and the eluted was collected into a 15mL falcon with 1mL of PBS. 1mL of RPMI 164 medium

containing 5% fetal bovine serum and 0.2% sodium azide were added to all the falcon with the samples.

Samples were prepared as previously described (115). Initially, an 8% ammonium chloride solution was used to lyse the erythrocytes in the samples. Subsequently, cells were resuspended in RPMI 164 medium containing 5% fetal bovine serum and 0.2% sodium azide. Cell suspensions, adjusted at $5x10^5$ cells per tube, were incubated for 30 min at 4°C with a defined combination of the labeled antibodies (listed below). Finally, cells were washed twice and resuspended in PBS. Twenty thousand events were acquired for each sample.

For staining, all antibodies were previously titrated to define correct working dilutions. Furthermore, isotype matched controls were included for each labeling. The following fluorochrome labeled antibodies were used in various combinations: anti-mouse CD21/CD35 PE (clone eBio4E3 eBioscience), anti-mouse CD138 APC (clone 281-2, BioLegend), anti-mouse FoxP3 eFluor660 (clone FJK-16s, eBioscience), anti-RORgamma PE (clone 4G419, Abcam), anti-mouse CD25 PE (clone PC61.5, Abcam), anti-mouse CD4 FITC (clone GK1.5, Abcam), anti-mouse B220 Fluorescein isothiocynate (FITC) (clone RA3-6B2, eBioscience), anti-CD19 APC (clone MB19-1, eBioscience), anti-CD24 FITC (clone M1/69, eBioscience), anti-GL7 PE (clone GL-7, eBioscience), anti-mouse IgD APC (clone 11-26c, eBioscience), anti-mouse IgM APC (clone RMM-1, BioLegend), mouse IgG1k isotype control PE (clone P3.6.2.8.1 eBioscience), mouse isotype control IgG2bk FITC (clone eBMG2b, eBioscience).

B cell subsets were defined as plasma cells ($B220^{low/-}IgD^-CD138^+$), naïve ($B220^+IgD^+$), memory ($B220^+IgD^-$), immature/transitional ($CD19^+CD21^+CD24^+$), germinal center ($GL7^+IgM^-$). T cell subsets were defined as Treg ($CD4^+CD25^+FOXP3^+$) and Th17 ($CD19^-CD4^+Rorgamma^+$).

Staining for Treg cells was performed as previously described (115): leukocytes from spleen and bone marrow were incubated at 4°C with CD4-FITC and CD25-PE antibodies for 30 minutes, then cells were washed and incubated for 10 minutes in the fixation/permeabilization solution

(FOXP3/transcription factor staining buffer set, eBioscience) in the dark at room temperature. Then cells were washed twice and incubated with FOXP3-eFluor660 antibody for 30 minutes at 4°C in the dark. After incubation, cells were washed twice and resuspended in PBS for the final acquisition.

For RORgamma intracellular staining was performed as previously described (116): cells were previously labeled with an anti-CD4-FITC, and then washed twice and permeabilized using the fixation/permeabilization solution (FOXP3/transcription factor staining buffer set, eBioscience) in the dark at room temperature. Then cells were washed twice and incubated with RORgamma PE antibody for 30 minutes at 4°C in the dark. After incubation, cells were washed twice and resuspended in PBS for the final acquisition. As a control, an appropriate isotype-matched negative control was added in order to distinguish between specific and non-specific labeling.

Analysis were carried out using CyFlow Space (Sysmex) and analyzed by FlowMax software (Partec GmbH, Münster, Germany).

Immunofluorescence and confocal microscopy

For indirect immunofluorescence (IF), cells were fixed in 2% paraformaldehyde for 20 min, permeabilized with 0.5% Triton X-100 in PBS for 15 min and treated with 0.05 mol/l NH_4Cl for 15 min. All steps were performed at room temperature (RT). Subsequently, cells were stained for PTX3, histone 3 (H3), C1q and mouse IgG.

The primary and secondary antibodies were diluted in PBS containing 0.5% BSA. Both primary and secondary antibodies were incubated at 37°C for 1 hour. All secondary antibodies were diluted 1:400.

For colocalization, diverse combination of the antibodies were used. PTX3 was visualized using a 1:200-diluted polyclonal antibody rabbit anti-mouse PTX3 (#GTX45054, GeneTex), followed by a Alexa 594-conjugated goat anti-rabbit IgG (#A-11037, LifeTechnologies) or by a 647-conjugated goat anti-rabbit IgG (#SCJ4600048, CF^{TM}647, Sigma-Aldrich) for confocal microscopy or IF,

respectively. H3, staining for nuclear material, was detected with a 1:600-diluted goat anti-mouse H3 (ab11946, Abcam), followed by a 488-labelled rabbit anti-goat IgG (#F7367, Sigma-Aldrich) or by a Alexa 594-labelled donkey anti-goat IgG (#A-11058, ThermoFisher) for confocal microscopy or IF, respectively. C1q was detected using a 1:100-diluted rat anti-mouse C1q antibody (ab11861, clone 7H8, Abcam), followed by a 488-labelled goat anti-rat IgG (# F6258, Sigma). IgG deposits were seen adding only a secondary antibody, 1:500 diluted, 488-labelled goat anti-mouse IgG (#F0257, Sigma).

Secondary antibodies were also used in the absence of primary antibodies in order to assess non-specific binding.

For IF analysis, the cell nuclei were labelled with 1.5 µg/ml Hoechst 33258 (Sigma-Aldrich) for 10 min at RT. For confocal analysis, DNA was stained using DRAQ5TM (Abcam). Finally, the slides were mounted with Mowiol anti-fade solution (Sigma-Aldrich). Leica DMI6000CS fluorescence microscope (Leica Microsystems) was used and samples were analysed using differential interference contrast (DIC) and fluorescence objectives. Images were acquired at 63x/1.4 oil objective magnification. Samples retrieved from the same mice were also analysed by confocal microscopy (Leica TCS SP8, Leica Microsystems) with a z-interval of 3 µm using a 100x/1.4 oil immersion lens (image size 1024x1024 pixel). Images were acquired using a DFC365FX camera and processed using the Leica Application Suite (LAS-AF) 3.1.1. software (Leica Microsystems).

Immune-electron microscopy (IEM) and immunogold

Thin cuts of kidney samples were fixed in 4% Paraformaldehyde (PFA) in sodium cacodylate buffer 0.1M pH, kept at 4°C overnight, then washed 3 times, ethanol dehydrated and embedded in LR White resin for 24 hours at 56° C. 80 nm thin sections were picked up onto 200 mesh nickel grids and the nonspecific antigenic sites were blocked for 1 hour at RT with a blocking solution made of BSA1% and Tween20 0.05% in 1×PBS. The grids were then labelled with the primary antibody

(rabbit anti-PTX (#GTX45054, GeneTex), 1:10) diluted in the blocking solution overnight at 4° C. The next day, grids were washed 5 times for 5 minutes each in PBS 1x and incubated with the secondary gold labelled antibody (anti-rabbit IgG 15 nm gold conjugated 1:75), and subsequently washed 5 times for 5 minutes each in PBS 1x, fixed in GA 2% in PBS 1x for 10 minutes and finally washed 3 times for 5 minutes each with double distilled water. To visualize deposits of IgG, anti-mouse IgG 15 nm gold conjugated (1:50) was used. Images were analysed by transmission electron microscope (FEI Tecnai G12) at 100 kV and acquired via Olympus Veleta camera at 4 megapixels.

Statistical analysis

The differences between groups were analyzed using Mann-Whitney U test for nonparametric continuous variables. Flow cytometry data were analyzed by FlowMax (Partec GmbH, Münster, Germany). Colocalization at IF was analyzed by Pearson's correlation coefficient (Rr). Presence of EDD at IEM was quantified according to a semiquantitative score (117) and Chi-squared test was used for comparison of histological and ultrastructural findings. A p value <0.05 was considered statistically significant.

Ethics

Use, treatment and sacrifice of mice was approved by the National Institutional Animal Care and Use Committee (Paper I and Paper II). Ongoing unpublished data got approval by the Italian Ministry of Health (authorization nr. 720/2107 PR.). Study on human samples (Paper III) was approved by the local ethics committee of the Charité Universitätsmedizin Berlin for research on B cells in autoimmune diseases. The collection of data and publication of results have been performed so as to guarantee anonymity of the patients.

RESULTS

In the following sections results of different papers are summarized, representing a progressive step-forward process.

Paper I

In this paper we investigated whether the restoration of the SERPINB3 pool in two lupus-prone strains would impact on disease course. Both preventive and therapeutic approach were evaluated in one strain.

Antibodies and proteinuria

We found significant difference in time of onset and serum levels (OD) of nephritogenic antibodies (anti-C1q and anti-dsDNA) in both NZB/WF1 and Mrl/lpr mice treated with SERPINB3 before proteinuria occurrence (preventive approach), which interestingly was maintained also in NZB/WF1 mice treated with a true therapeutic approach *(*NZB/W F1 mice: difference in anti-C1q levels, group 1 vs. group 2**:** weeks 21, 25, 28 and 32 ($p < 0.0001$ for all time points); difference in anti-dsDNA levels, group 1 vs. group 2 weeks 21, 25, and 28 ($p < 0.0001$ for all); difference in anti-C1q levels, group 3 vs. group 4 at week 28 ($p = 0.002$); difference in anti-dsDNA levels, group 3 vs. group 4 at weeks 28 and 32 ($p < 0.0001$ for both). *Mrl/lpr mice*: difference in anti-C1q levels, group 5 vs. group 6 at weeks 15 ($p=0.011$) and 18 ($p=0.001$); difference in anti-dsDNA antibodies group 5 vs. group 6 at weeks 12 ($p<0.0001$), 15 ($p=0.006$) and 18 ($p=0.046$)). No differences in serum creatinine levels were found in either group.

Proteinuria levels (mg/dl as median (min-max)) were significantly lower and appeared later in time in mice prophylactically treated with SERPINB3 belonging to both strains. Difference of proteinuria between group 1 and group 2 was significant at weeks 21 ($p=0.023$), 23 ($p=0.001$) and 29 ($p=0.036$);

difference between group 5 and group 6 was significant at weeks 12 (p=0.001) and 18 (p=0.008) (**Table 3)**.

Table 3. Comparison of proteinuria between SERPINB3-treated and vehicle-treated NZB/NZW F1 mice (preventive and therapeutic approaches) and MRL/lpr mice

Preventive approach			
	SERPINB3-treated	**vehicle-treated**	**p**
Week 17	0 (0-0)	0 (0-0)	n.s.
Week 21	0 (0-0)	15 (0-15)	0.023
Week 23	0 (0-0)	15 (0-2000)	0.001
Week 25	15 (0-100)	23 (15-2000)	n.s.
Week 27	30 (15-300)	2000 (15-2000)	n.s.
Week 29	65 (15-300)	2000 (100-2000)	0.036
Week 33	300 (30-2000)	2000 (300-2000)	n.s.
Therapeutic approach			
Week 17	0 (0-0)	0 (0-0)	n.s.
Week 21	0 (0-15)	0 (0-0)	n.s.
Week 23	30 (15-30)	15 (0-15)	0.010
Week 25	30 (30-100)	15 (0-300)	0.045
Week 27	100 (100-100)	15 (0-300)	n.s.
Week 29	100 (15-2000)	165 (15-2000)	n.s.
Week 33	30 (15-2000)	300 (100-2000)	n.s.
MRL/*lpr* mice (prophylactic approach)			
w9	0 (0-0)	0 (0-0)	n.s.
w12	15 (0-30)	100 (15-100)	0.001
w15	100 (30-300)	100 (100-300)	n.s.
w18	100 (100-2000)	300 (300-2000)	0.008

Regarding NZB/WF1 mice undergoing therapeutic approach (i.e. after occurrence of proteinuria≥100mg/dl), a delay and decrease in proteinuria levels was apparent starting from week 29, yet not reaching statistical significance. At the 25th week of age, 40% of mice of group 3 (SERPINB3 treated) showed proteinuria levels ≥300 mg/dl vs. 100% of mice of group 4 (controls).

Survival rates

Proteinuria-free survival (proteinuria <300 mg/dl) and overall survival rates were compared only in NZB/W F1 mice followed until natural death and were found to be higher in mice treated with SERPINB3 with either a preventive or a therapeutic approach.

In fact, at the 31st week of age, 50% of mice in group 1 had proteinuria levels ≥300mg/dl, compared with 90% in group 2; the last mouse of group 1 developed proteinuria ≥300 mg/dl at the 44th week of age and the last of group 2 at the 33rd week of age, with an overall significantly longer proteinuria-free survival in group 1 vs. group 2 (median 25°-75°: 31 weeks (30-41.50) vs. 26.50 (23.75-30.75) p=0.002). Consistently, global survival rate was significantly higher in group 1 than in group 2 mice (median 25°-75°: 38 weeks (34-40) vs. 29 weeks (29-33), p=0.001) (**Figure 1A, 1B).**

Similarly, proteinuria-free survival and overall survival rates were significantly higher in group 3 than in group 4 (p=0.014 and p=0.009, respectively) (**Figure 1C, 1D**).

Figure 1. Survival rates in SERPINB3- and PBS-treated mice.

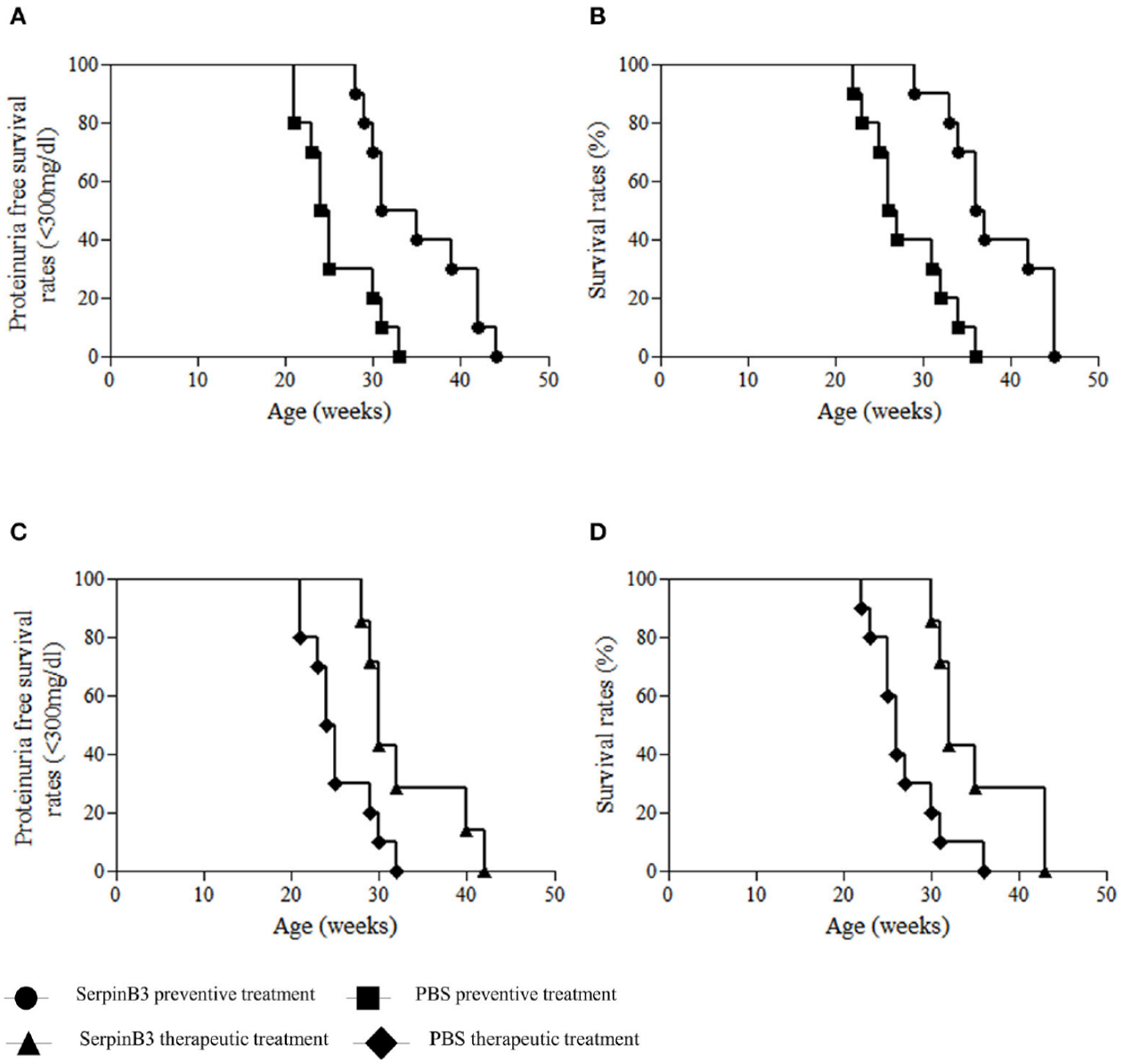

Proteinuria-free and overall survival in NZB/WF1 mice treated with preventive (A,B) or therapeutic approach (C,D). Mantel-Cox test.

***Footnotes**: NZB/W F1: New Zealand Black/White F1 mice; SERPINB3: Serin protease inhibitor B3; PBS: phosphate buffer saline*

Histological analysis

Only kidneys harvested from mice sacrificed at given timepoints were included in the analysis.

Among MRL/*lpr* mice sacrificed at week 13, no significant difference was found in glomerular, tubular or interstitial lesions between treated and control mice, though the percentage of mice showing severe glomerular lesions (score 4-5) was higher in group 6 vs. group 5 (33% vs. 0).

Among MRL/*lpr* mice sacrificed at week 16-18, severe tubular lesions (score 4) were found to be significantly more prevalent in group 6 vs. group 5 ($p=0.014$). Severe glomerular lesions were found to be less prevalent in group 5 vs. group 6 (75% vs. 100%) though no statistical significance was reached. No difference was found in severity of perivascular inflammation.

Concerning NZB/WF1 mice sacrificed at week 27, prevalence of severe glomerular and tubular lesions were comparable among group 1 and group 2.

Figure 2 shows representative kidney images with various degrees of severity.

Th17/treg distribution among splenocytes of MRL/lpr mice

Flow-cytometry analysis showed a remarkable increase in Treg cells among T lymphocytes isolated from spleen of SERPINB3-treated MRL/lpr mice that was significantly higher than in controls at week 13 (% mean±SD: week 13: serpin 2.1%±0.05 vs. PBS 1.4%±0.01, $p < 0.0001$; Week 16: serpin 5.2±0.7 vs. PBS 3.2±0.8). These findings were associated with a parallel decrease in Th17 cell number (% mean ± SD: week 13: serpin 0.5±0.01 vs. PBS 1.7±0.05, $p < 0.0001$; week 16 serpin 1.8± 0.8 vs. PBS 4.8±1.2), resulting in a significant reduction in the Th17:Treg cell ratio in SERPINB3-treated mice compared with PBS-treated mice (**Figure 3**).

Figure 2. Representative kidney samples with various degrees of severity

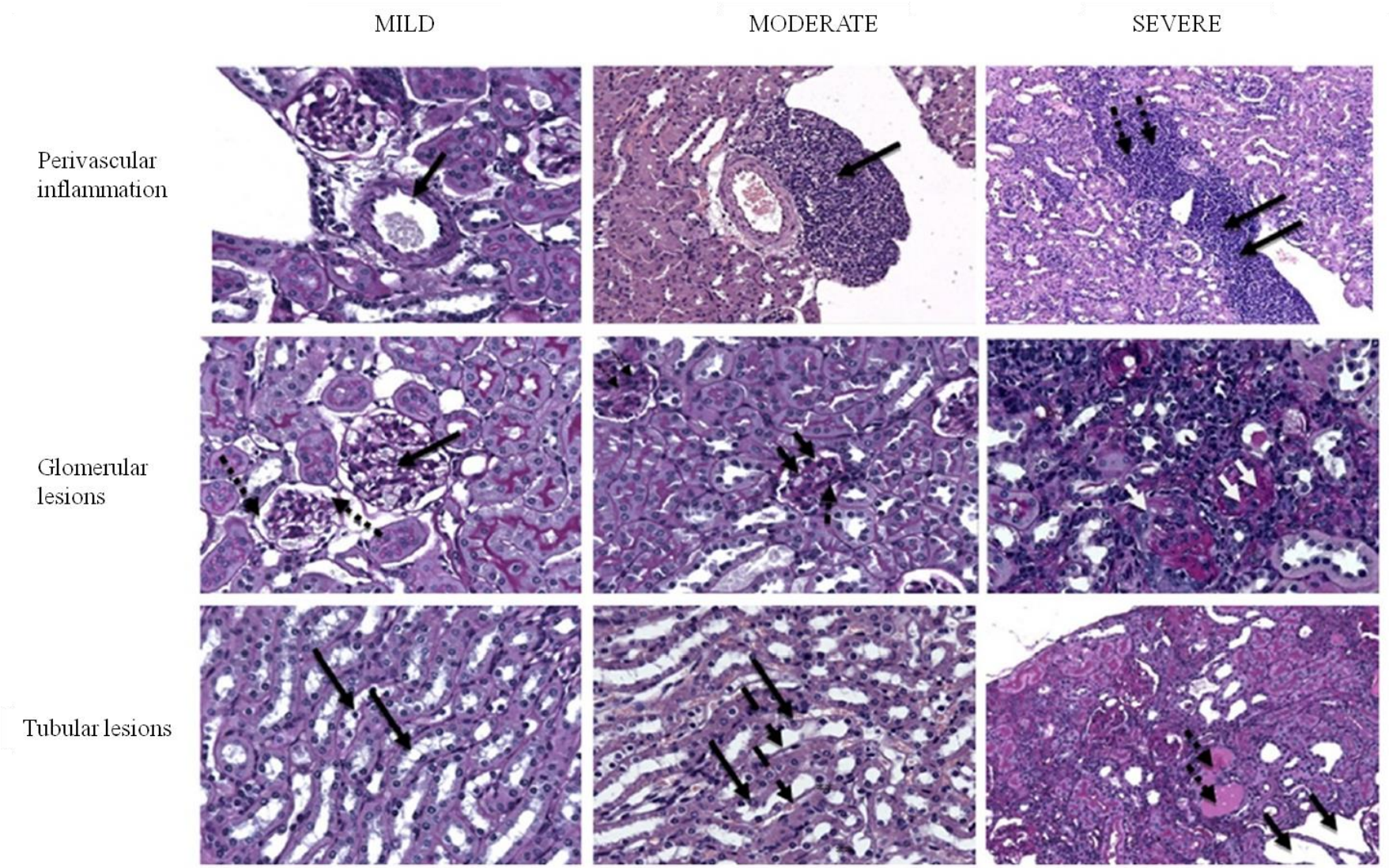

Representative images of mouse kidney with different extent of perivascular lesions (upper row), glomerular lesions (middle row) and tubular lesions (lower row). Upper row, left to right: normal vasculature with patent artery and clear renal vein (magnification PAS40x), indicated by thick arrow; grade 3 infiltrate partially surrounding the renal artery and bulging into the adjacent vein with sparing of connective tissue (HE20x), indicated by thick arrow; grade 5 perivascular infiltrate fully surrounding the arcuate artery and invading both the vein (thick black arrows) and the adjacent connective tissue (thick dotted black arrows) (HE10x). Middle row, left to right: near normal glomeruli (thick black arrows) with preserved basement membrane and urinary space (thick dotted black arrows) (PAS40x); intermediate damaged glomeruli with reduced urinary space, thickened basement membrane (thick black arrows), cellular hyperplasia (thick dotted black arrows) and initial septal fibrosis (thin dotted black arrows) (PAS40x); advanced glomerular damage with disappearance of glomerular structure, glomerular collapse and diffuse glomerulosclerosis (two white thick arrows; single arrows pinpoints absence of urinary space due to collapse). Diffuse lymphocytic infiltrate is also present (PAS40x).

Lower row, left to right: near normal renal tubuli at the medullo-cortical interface with normal cell nuclei in a wide cytoplasm (thick black arrows) (PAS40x); initial tubular dilation with flattened epithelial cells (thick dashed black arrows) with nuclei bulging into the tubular space (thick black arrows) (magnification PAS40x); severely dilated tubuli (thick black arrows) with loss of normal architecture and widely represented protein casts (pink lakes) (thick dotted black arrows) (PAS10x).

***Footnotes**: PAS, periodic acid of Schiff; HE, hematoxylin-eosin.*

Figure 3. Th17/Treg ratio decreases among mice treated with SERPINB3

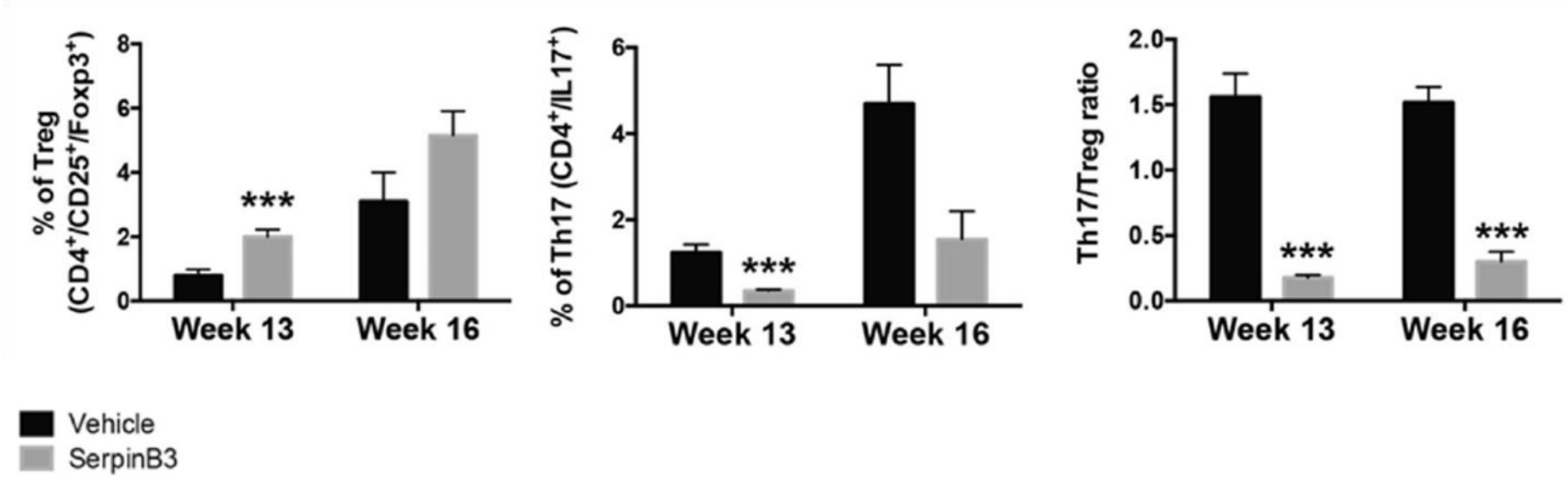

*Left to right. Proportion of Treg on total pool of CD4+, week 13 to week 16. Proportion of Th17 on total pool of CD4+, week 13 to week 16. Ratio of Th17 cells to Treg cells (n = 3 per group). Results are the mean ±SD. ***p < 0.0001 vs. vehicle-treated controls.*

***Footnotes**: Th, T helper cells; Treg, regulatory T cells.*

In summary, we found that restoration of SERPINB3 pool in lupus-prone mice may improve disease course following either a preventive or therapeutic approach. Focusing on renal involvement, this appears to be milder in treated mice versus controls, as both nephritogenic antibodies and proteinuria occurrence are delayed in time and lower in titers/amount among treated mice. These data are not yet conclusive especially regarding the mechanistic pathway by which SERPINB3 could affect renal inflammation, however it suggests that abnormalities in homeostatic pathways in SLE might affect disease development and may be counteracted by a therapeutic rebalance of those pathways.

Paper II

Descending from clinical findings that showed an inverse correlation between anti-PTX3 antibodies and occurrence of LN among SLE patients, as well as a direct correlation between renal PTX3 deposition and proteinuria and renal fibrosis (108-111), we replicated an immune reaction against PTX3 by immunizing lupus-prone NZB/WF1 mice with hrPTX3 and compared them with controls immunized with placebo in order to assess any clinical changes in disease course provided by rise in anti-PTX3 antibodies.

Antibodies and proteinuria

First, we demonstrated that anti-PTX3 antibodies arose around week 22 only in mice immunized with this molecule following a vaccine-like reaction, while anti-dsDNA and anti-C1q antibodies were delayed and at lower titre in PTX3-group versus control groups. In fact, anti-C1q antibodies were detected in PTX3-immunized mice from the 22nd week of age, while in group 2 from the 17th week of age. Difference in anti-C1q levels was statistically significant at weeks 14 ($p=0.002$), 17 ($p=0.015$) and 22 ($p=0.002$). Likewise, group 1 mice developed anti-dsDNA antibodies later

and at significantly lower levels than control mice and difference between group 1 and group 2 were significant at week 14 ($p < 0.0001$), 17 ($p < 0.0001$), 22 ($p < 0.0001$), 28 ($p= 0.028$), 35 ($p = 0.016$). Notably, anti-dsDNA antibodies in group 1 started to rise as soon as anti-PTX3 started to decrease.

Furthermore, proteinuria occurrence was delayed and reduced in PTX3 immunized mice, being significantly lower than in controls from week 26 to week 33 (**Table 4**).

Table 4. Comparison of circulating autoantibody levels and proteinuria levels between Group 1 (PTX3, alum, and PBS) Group 2 (alum and PBS), Group 3 (PBS) mice. Antibodies are expressed as the median (minemax) of the mean OD of the double of every serum, proteinuria in mg/dl as median (minemax) and serum creatinine in mmol/L as median (min-max).

Anti-PTX3					
Week 11	0.014 (0.006-0.067)	n.s.	0.021 (0.002-0.049)	n.s.	0.037 (0.008-0.067)
Week 14	1.029 (0.408-1.990)	<0.0001	0.061 (0.039-0.168)	n.s.	0.030 (0.017-0.061).
Week 17	1.794 (1.624-2.982)	<0.0001	0.094 (0.044-0.160)	n.s.	0.022 (0.003-0.106).
Week 22	2.201 (1.265-2.591)	<0.0001	0.039 (0.015-0.149)	n.s.	0.028 (0.005-0.129)
Week 28	0.451 (0.121-2.036)	<0.0001	0.049 (0.015-0.138)	n.s.	0.023 (0.150-0.189)
Week 35	0.300 (0.010-0.915)	n.s.	0.047 (0.039-0.082)	n.s.	0.023 (0.019-0.073)
Anti-C1q					
Week 11	0.114 (0.105-0.189)	n.s.	0.183 (0.103-0.216)	n.s.	0.100 (0.073-0.145)
Week 14	0.165 (0.133-0.197)	0.002	0.228 (0.184-0.297)	n.s.	0.193 (0.119-0.281)
Week 17	0.207 (0.149-0.360)	0.015	0.315 (0.190-0.397)	n.s.	0.333 (0.261-0.383)
Week 22	0.368 (0.237-0.484)	0.002	0.494 (0.422-0.951)	n.s.	0.553 (0.398-0.751)
Week 28	0.609 (0.543-0.967)	n.s.	0.701 (0.528-1.214)	n.s.	0.845 (0.568-1.259)
Week 35	0.853 (0.688-1.314)	n.s.	1.222 (0.795-1.862)	n.s.	1.427 (1.357-1.498)
Anti-dsDNA					
Week 11	0.033 (0.020-0.061)	n.s.	0.082 (0.014-0.129)	n.s.	0.092 (0.003-0.142)
Week 14	0.043 (0.022-0.130)	<0.0001	0.135 (0.105-0.196)	n.s.	0.157 (0.071-0.203)
Week 17	0.100 (0.050-0.131)	<0.0001	0.224 (0.202-0.263)	n.s.	0.265 (0.191-0.498)
Week 22	0.168 (0.113-0.216)	<0.0001	0.328 (0.304-0.359)	n.s.	0.355 (0.305-0.489)
Week 28	0.252 (0.126-0.564)	0.028	0.434 (0.364-0.824)	n.s.	0.464 (0.427-0.967)
Week 35	0.326 (0.216-0.534)	0.016	0.549 (0.537-0.581)	n.s.	0.593 (0.561-0.626)
Proteinuria					
Week 19	0 (0-0)	n.s.	0 (0-15)	n.s.	0 (0-15)
Week 22	15 (15-30)	n.s.	30 (0-30)	n.s.	30 (15-30)
Week 26	15 (15-30)	0.008	30 (15-100)	n.s.	30 (30-30)
Week 28	30 (15-100)	0.002	200 (30-2000)	n.s.	300 (100-2000)
Week 30	100 (30-100)	<0.0001	300 (100-2000)	n.s.	300 (100-2000)
Week 33	100 (30-300)	0.0002	300 (300-2000)	n.s.	300 (300-2000)
Week 35	300 (100-2000)	n.s.	2000 (300-2000)	n.s.	2000 (300-2000)
Serum Cr					
Week 11	7 (4-9)	n.s.	3 (2-7)	n.s.	NA
Week 22	5 (3-8)	n.s.	6 (2-6)	n.s.	NA
Week 28	19 (5-25)	n.s.	34 (7-57)	n.s.	31 (6-52)
Week 35	17 (5-51)	n.s.	26 (7-126)	n.s.	33 (32-61)

Survival rates

Proteinuria-free survival was increased in group 1 compared to controls (median 25°-75°: 31 weeks (28.50-36) vs. 29 (28-30), p=0.037) (**Figure 4A).** At the 35th week of age, 60% of mice in group 1 had proteinuria levels >300 mg/dl compared with 90% in group 2; the last mouse of group 1 developed proteinuria>300 mg/dl at the 39th week of age and the last of group 2 at the 36th week of age.

Global survival rate was also significantly higher in group 1 than in group 2 and group 3 (median 25°-75°: 36.50 (33.25-39.25) vs. 33 (30-35), p= 0.030) (**Figure 4B**). In group 2, 50% of mice died within the 30th week of age vs. 20% of PTX3-immunized mice. At the 34th week of age, 70% of group 1 mice were still alive vs. 30% of group 2 mice. When the last mouse of group 2 died, only 60% of PTX3-immunized mice were dead.

Figure 4. Proteinuria-free and overall survival rates in PTX3-immunized, alum- and PBS-injected mice

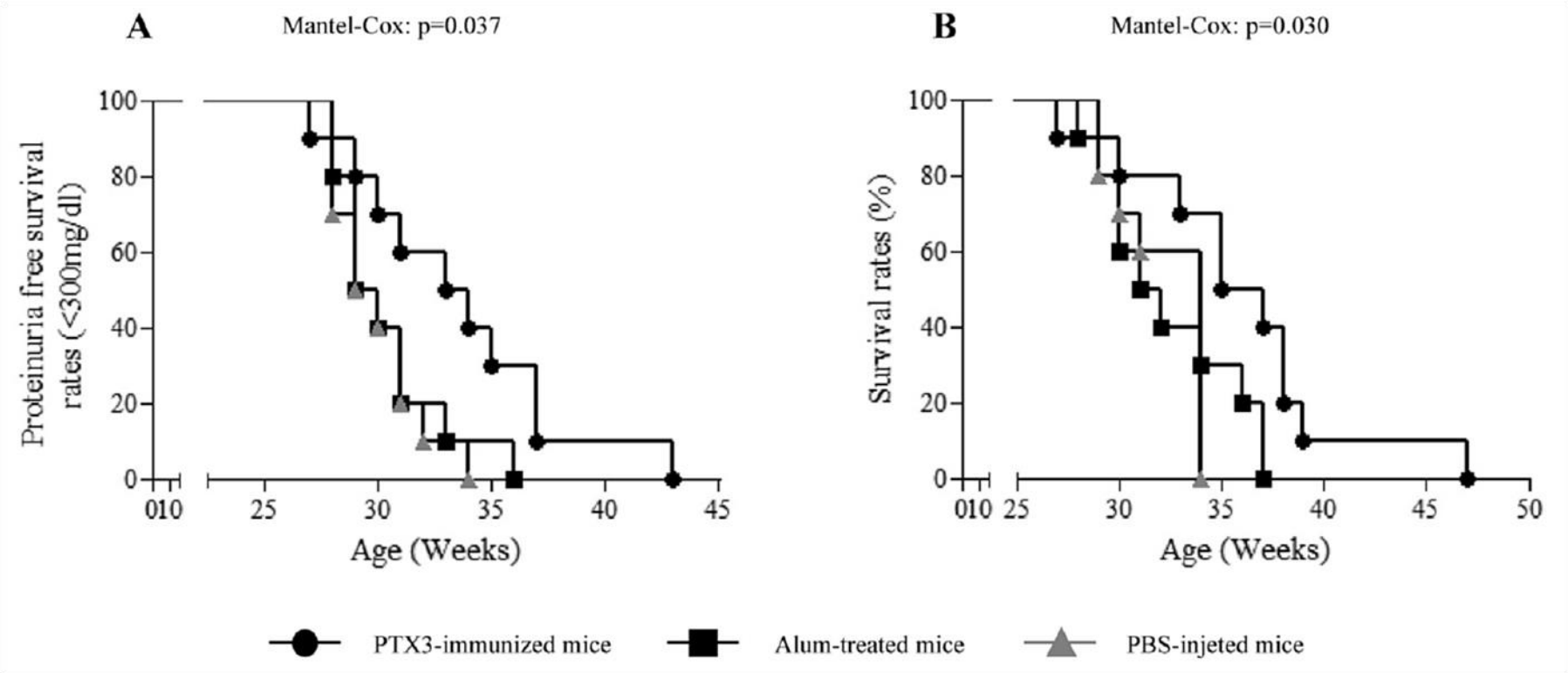

Proteinuria-free survival rates (<300 mg/dl) (A) and overall survival rates (B) were significantly longer in PTX3-immunized vs. alum-treated and PBS-injected mice.

***Footnotes**: PTX3-immunized mice: mice immunized with the long pentraxin 3, PBS-injected mice: mice injected with phosphate buffered saline.*

No differences in serology, renal function or survival was found between group 2 and 3, suggesting that adding alum is not required in case of immunization with PBS.

Interestingly, data on human sera revealed that a high proportion of the IgG anti-PTX3 pool is made of IgG4 antibodies, suggesting that this may be a reason why they do not bear a pro-inflammatory potential. Anti-PTX3 antibodies from patient sera at various concentrations bound immobilized PTX3 forming PTX3-anti-PTX3 immune complexes, that were in turn bound by C1q in a dose-dependent fashion, yet to a lesser extent than the C1q binding obtained with commercial affinity-purified IgG anti-PTX3 antibodies at the same antibody concentration (**Figure 5).**

The study was not conceived to compare histological findings, however kidneys were harvested at death of mice in either group and comparison of histology at light microscopy and immunohistochemistry showed an increased deposition of PTX3 across glomeruli and tubuli of control mice, with a greater prevalence of mesangial hypercellularity and proliferation, leukocyte infiltration, thickening of the glomerular capillary walls, cellular crescents and glomerular scarring within groups 2 and 3 versus group 1.

Figure 5. Effect of anti-PTX3 antibodies on the interaction of C1q with solid-phase immobilized PTX3

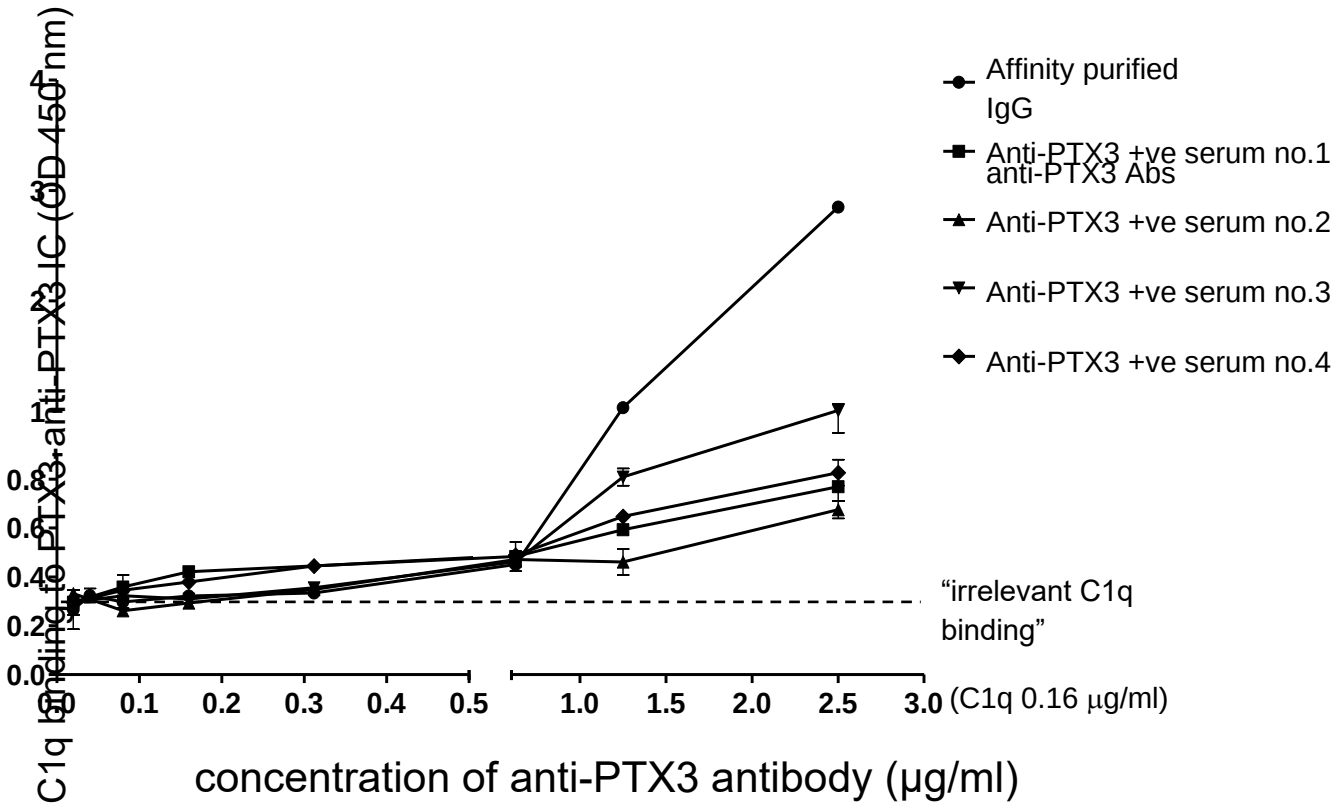

Microtiter wells coated with PTX3 (5 µg/ml) were incubated with a fixed concentration of C1q (0.16 µg/ml/1%BSA/PBS) or with a mixture of C1q and antibodies, consisting of C1q (0.16 µg/ml/1%BSA/PBS), together with commercial affinity-purified IgG anti-PTX3 antibodies, or the sera from four SLE patients with high anti-PTX3 antibody level, at increasing concentrations. C1q binding was detected and expressed as mean ± SD optical density values (OD 450 nm) of the duplicates for each sample. Data shown in figure are representative for three independent experiments.

***Footnotes**: PTX3-anti-PTX3 IC: immune-complexes made of pentraxin3 and anti-pentraxin3 antibodies.*

Paper III

In this study we aimed at characterizing PTX3-specific B cells circulating in blood of SLE patients with or without LN (biopsy-proven) and to compare levels and distribution of B subpopulations among patients and HD. Demographics and clinical features of patients and HD are summarized in **Table 5).** The patient pool showed a uniformity in treatment and steroid dosage.

The first result is the development of an original flow-cytometry assay which allowed the identification of B cells which were most likely to be specific for PTX3. In fact, no B cell receptor for PTX3 binding was characterized so far, therefore we performed blocking experiments with unlabeled PTX3 pre-incubated with lysed blood from patients and controls, and just analyzed the amount of B cells which could be substantially blocked by unlabeled PTX3, assuming that the block could stand for a specific binding (**Figure 6A and 6B**).

Table 5. Demographic and therapeutic features of healthy donors and patient groups

	Healthy donors	Patients	
		Non renal SLE	LN
No.	22	26	12
Mean age ±SD	33.4±8.6	34.6±10.2	41.8±10.37
Female (%)	77.2	84.6	75
Active disease (cSLEDAI≥2) (%)		3/26 (11.5%)	7/12 (58.3%)
cSLEDAI [mean±SD]		1.14±3.66	4.17±3.86
LN class* (no.) Proliferative (III or IV) V or mixed		N/A**	 7 5
24-hours proteinuria (g) [mean±SD]		N/A	4±1.41
Active urinary sediment§ (%)		0	41.7
Concomitant treatment			
Oral prednisone (%) [mean dosage ±SD]		60.8 [4.04±4.14]	58.3 [3.98±6.05]
HCQ (%)		69.4	58.3
Immunosuppressants (%)		73.9	66.7
MMF		34.7	41.7
MTX		4.3	0
AZA		30.4	25

*International Society of Nephrology/Renal Pathology Society (ISN/RPS) 2003** these patients never underwent kidney biopsy due to lack of renal involvement; §>5 white blood cells and/or >5 red blood cells/high power field and/or heme-granular/red cell casts

Footnotes: SLE, systemic lupus erythematosus; LN, lupus nephritis; SD, standard deviation; cSLEDAI, clinical SLE disease activity index; HCQ, hydroxychloroquine; MMF, mycophenolate mofetil; MTX, methotrexate; AZA, azathioprine; N/A not available.

Figure 6. Identification of PTX3+ B cells among CD19+CD20+ B cells.

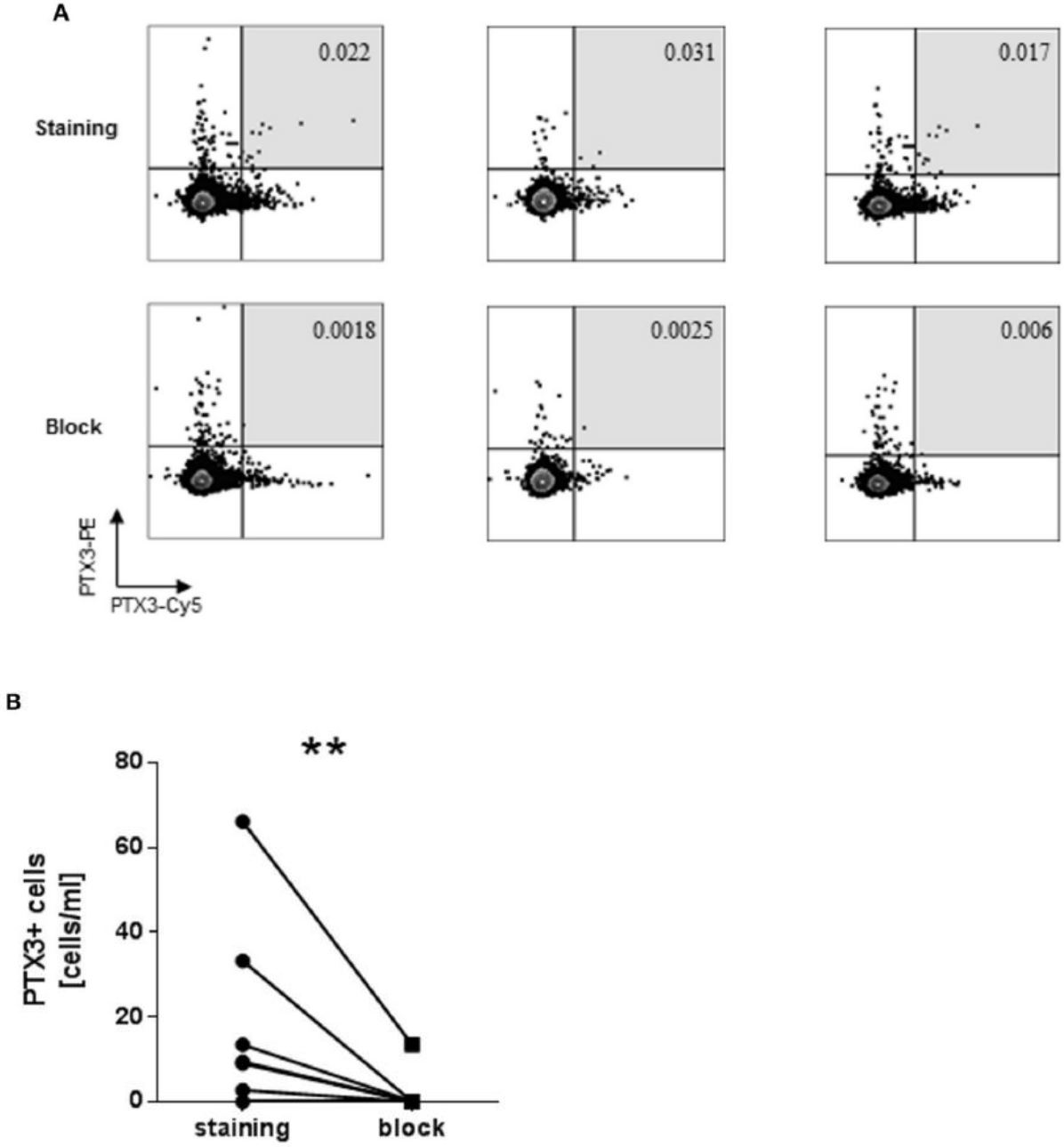

(A) *Three representative dot plots of the PTX3-specific B cells before and after blocking with unlabeled PTX3. Only B cells staining positive for both PTX3-Cy5 and PTX3-PE were considered (light gray square).* ***(B)*** *Quantification of PTX3 binding among B cells before and after blocking of PTX3.*

Footones*: Cy5, cyanin 5; PE, phycoerythrin. **<0.01.*

Flow-cytometry analysis showed a significant decrease in proportion and absolute number of $CD19^{+}PTX3^{+}$ B cells in patients with LN compared to both SLE and HD (mean±SD cells/ml: LN 0.023 ±0.027 vs. HD 33.09±48.15, p=0.008; LN 0.023±0.027 vs. non-renal SLE 12.53±20.24, p=0.033), which was maintained through the naïve ($CD20^{+}CD27^{-}$) and memory compartment ($CD20^{+}CD27^{+}$) (mean±SD naïve/ml: LN 0.18±0.58 vs. HD 30.12±42.96, p=0.0001; LN 0.18±0.58 vs. non-renal SLE 16.22±24.88, p=0.028; mean ±SD memory/ml: LN 0.97±2.18 vs. HD 12.75±24.88, p=0.011; LN 0.97±2.18 vs. non-renal SLE 4.07±5.21, p = 0.038) (F**igure 7A**). The frequencies of PTX3+ B cells and B cell subsets were consistently decreased in LN (**Figure 7B**), while there was no significant difference between HD and non-renal SLE. Of note, no difference in $PTX3^{+}$ naïve and memory compartment was identified between active and inactive LN (data not shown), suggesting that the actual decrease in LN is not related to disease activity, being rather an early event during disease commitment and be a typical feature of patients who will develop LN.

We detected nearly no circulating $PTX3^{+}$ plasmablasts ($CD27^{hi}CD20^{-/low}$) in whole blood sampled for the majority of donors, where a minimum of $1x10^{6}$ events was retrieved from each sample. These cells were absent even when a larger amount of cellular events ($27\ x10^{6}$) from an SLE patient among a total of 7,648 plasmablasts was analyzed.

Using CD27 and IgD as surface markers, we found that the majority of circulating PTX3+B cells resided among the $CD20^{+}CD27^{-}IgD^{+}$ mature pre-switch naïve subset, followed by a lower number of $CD20^{+}CD27^{+}IgD^{+}$ B cells (**Figure 7C**), likely representing pre-switched memory B (118). This distribution remained consistent among HD and non-renal SLE patients, while LN patients did not show any difference among B cell subsets (**Figure 7C**).

Figure 7. PTX3+ B cells distribution in SLE, LN and HD.

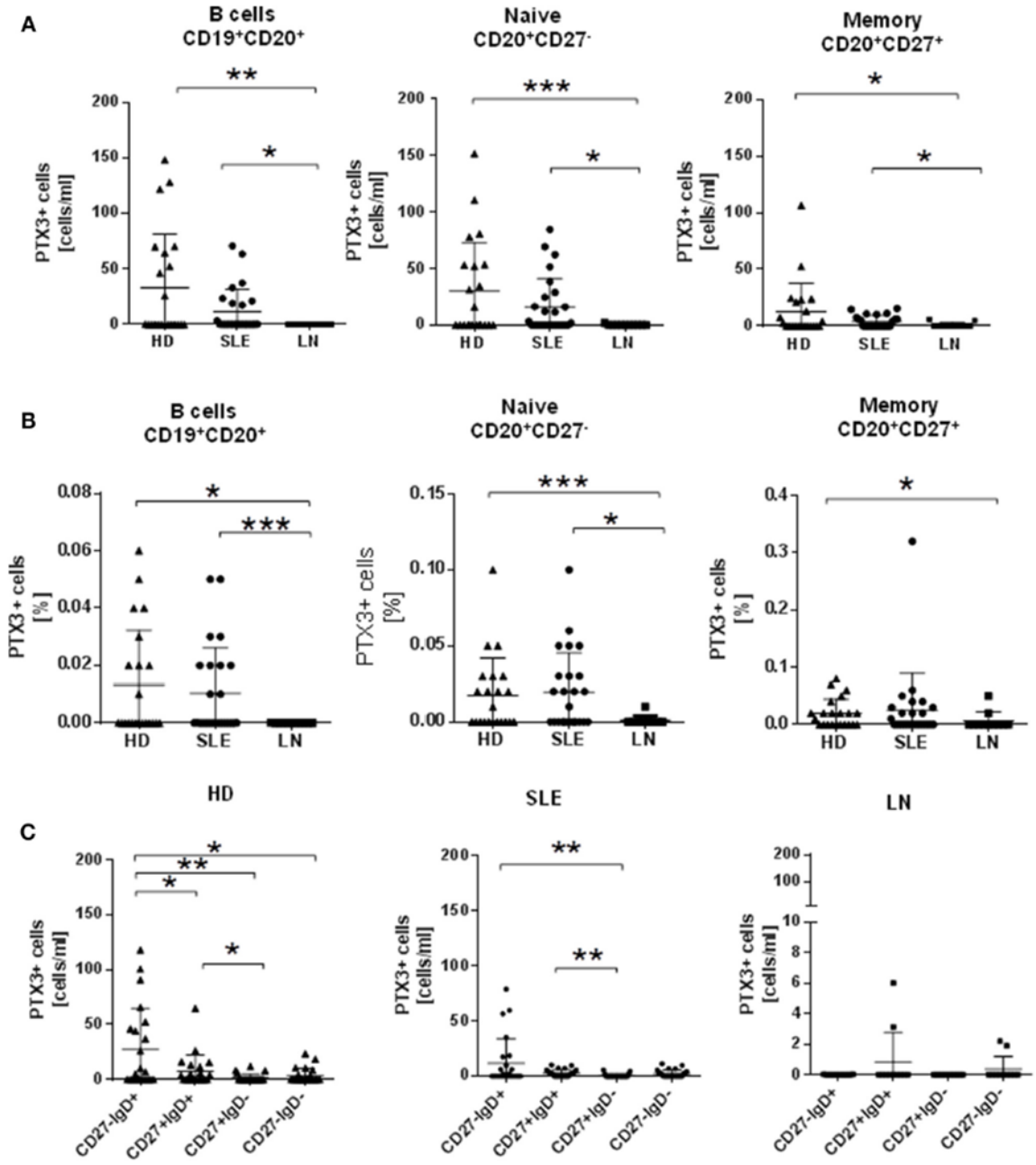

Figure 7. *PTX3+ B cells are decreased in patients with LN and are mainly confined to CD27−IgD+ B cells.* *A) Absolute numbers of PTX3+ B cells (cell/mL) within (left to right): total; naïve;) memory B cells in HD (n = 22), SLE (n = 26) and LN (n = 12). (B) Frequencies of PTX3+ B cells (left), naïve (middle), and memory (right) are decreased in LN (n = 12) in comparison with HD (n = 22) and SLE (n = 26). (C) Distribution of CD27 and IgD expression by PTX3+ B cell subsets. Enrichment in the naïve pool with decreases in the other subsets was found in HD (n = 22) and SLE (n = 26), but not in LN (n = 12). Mann-Whitney U-test (*< 0.05, **< 0.01, ***< 0.001).* ***Footnotes****: SLE, systemic lupus erythematosus; HD, healthy donors; LN, lupus nephritis; PTX3 pentraxin3.*

Paper IV (unpublished)

In light of obtained results certifying a clinical improvement upon immunization with hrPTX3 of lupus-prone mice (Paper II) and depicting remarkable difference between lupus patients with and without LN in terms of PTX3-specific B cell subsets (Paper III), the last part of the experimental process was aimed at exploring histological and ultrastructural findings within the kidneys of lupus prone NZB/W F1 female mice following immunization with hrPTX3 or PBS, according to the prophylactic protocol used in Paper II. Only mice immunized with PTX3 developed high levels of anti-PTX3 antibodies (**Figure 8**). Mice were sacrificed at given timepoints in order to be able to compare tissue samples consistently. Besides, flow-cytometry was also performed on harvested splenocytes and bone marrows.

Overall, 19 NZB/WF1 mice could undergo the programmed sacrifice, as 3 (two from the PBS group and one from the PTX3 group) died before the scheduled timepoint.

Figure 8. Serum levels of anti-PTX3 antibodies

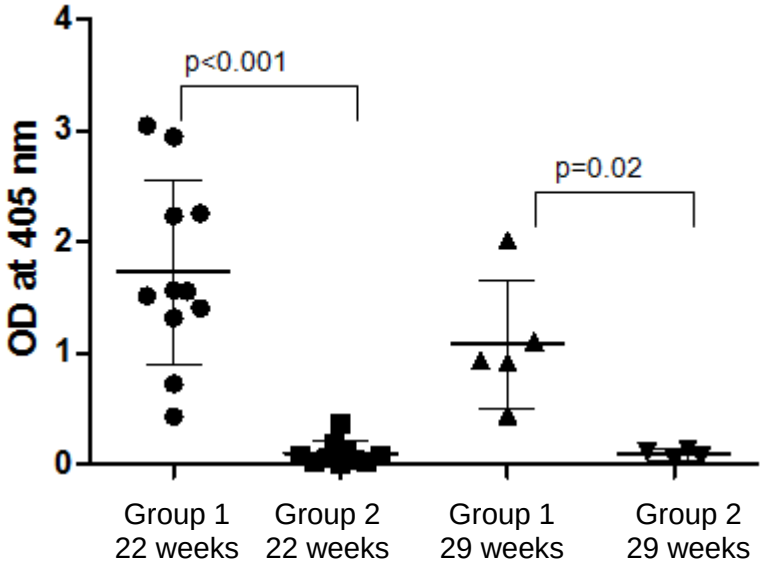

Only mice immunized with hrPTX3 develop detectable levels of anti-PTX3 antibodies, standing for an effective immunization. ***Footnotes****: OD, optical density*

IEM

Observations at IEM are so far available for 13 out of 19 mice belonging to both groups. IEM revealed a remarkable presence of widespread EDD in glomeruli of mice treated with PBS, mostly localized in the mesangium and in the GBM compared to nearly absence of EDD among mice immunized with PTX3 (**Figure 9**). In detail, 5 out of 7 (71%) PBS-injected mice showed severe EDD deposition, which were present only in 1/6 (17%) mice immunized with PTX3. Interestingly, PTX3-immunized mice sacrificed at 29 weeks still exhibited no or few EDD in comparison to PBS-treated mice sacrificed at a younger age (22 weeks), suggesting a long-lasting protective effect likely derived from the immunization. Moreover, 7 out of 7 (100%) PBS-injected mice had remarkable effacement of podocytes with flattening of foot processes which was seen only in 1 out of 6 (17%) PTX3-immunized mice (p=0.026) (**Table 6)**.

Notably, PTX3 was shown inside the EDD by immunogold **(Figure 10),** without measurable difference between PTX3-immunized and PBS-treated mice, suggesting PTX3 is a component of EDD regardless of their number and localization.

Age-matched lupus-prone mice show less glomerular EDD following immunization with PTX3.

22-weeks old lupus-prone mouse immunized with PTX3 (A) shows remarkably less glomerular EDD vs. age-matched PBS-treated mouse (B).

***Footnotes**: EDD, electron-desne deposits; GBM, glomerular basement membrane; RBC, red blood cell; PTX3, pentraxin3; PBS, phosphate buffer saline.*

Figure 9. EDD in lupus-prone mice immunized with PTX3 or PBS

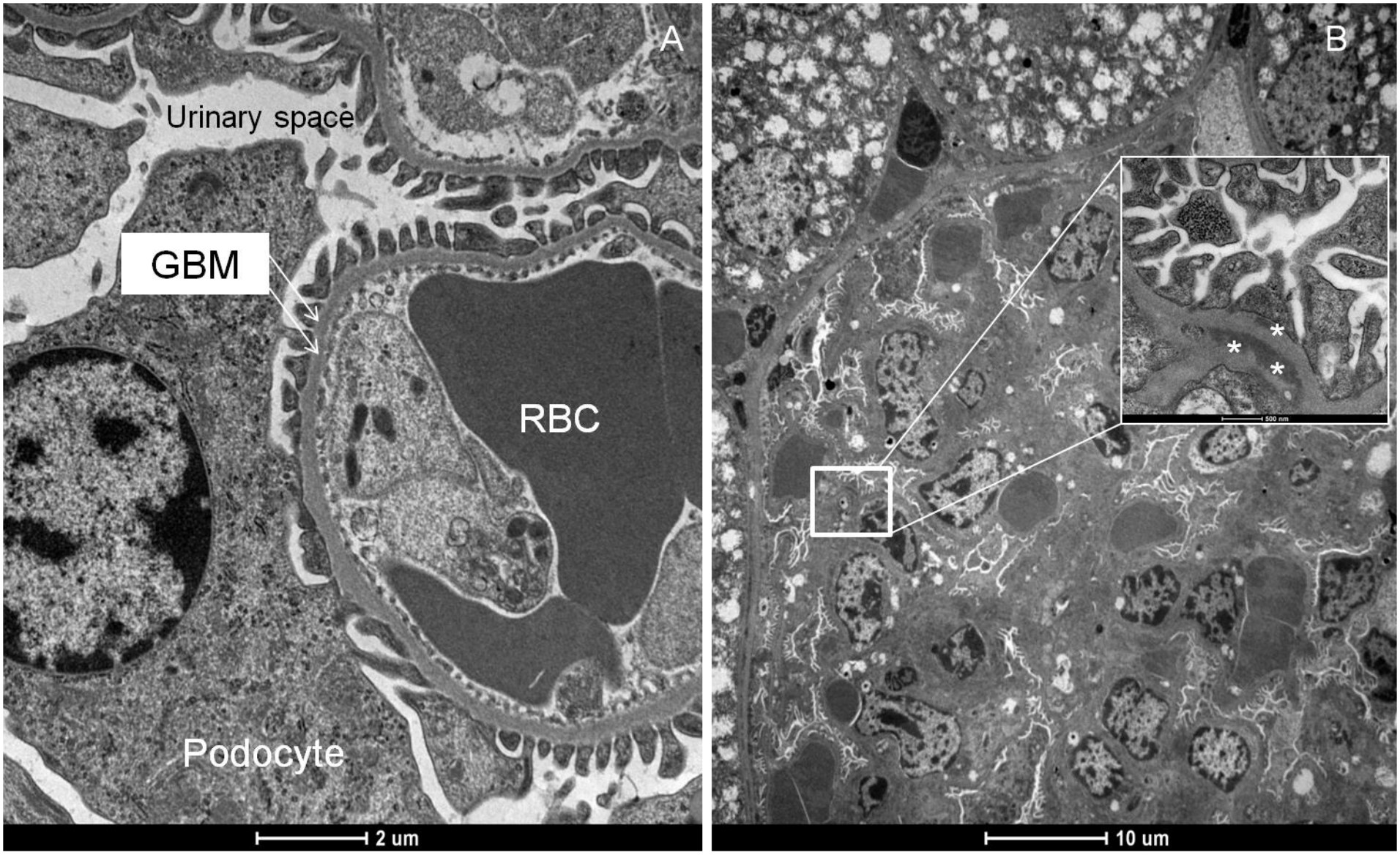

Table 6. Distribution of glomerular ultrastructural lesions among PTX3-immunized and PBS-treated mice

	EDD mesangium/GBM		Podocyte effacement	
PTX3 (n=6)	Score 0	4 (67%)	Score 0	5 (83%)
	Score 1	1 (17%)	Score 1	-
	Score 2	1 (17%)	Score 2	1 (17%)
PBS (n=7)	Score 0	2 (29%)	Score 0	-
	Score 1	1 (14%)	Score 1	3 (43%)
	Score 2	4 (57%)	Score 2	4 (57%)

PTX3: pentraxin 3, PBS: phosphate buffer saline; EDD: electron dense deposits; GBM: glomerular basement membrane.

EDD: Score 0: no EDD; Score 1: 1-3 EDD location; Score 2: >3 EDD locations
Podocyte effacement: Score 0: negative; Score 1: average of podocyte foot process width >1um; Score 2: absence of podocyte foot processes

Figure 10. PTX3 localization inside the EDD

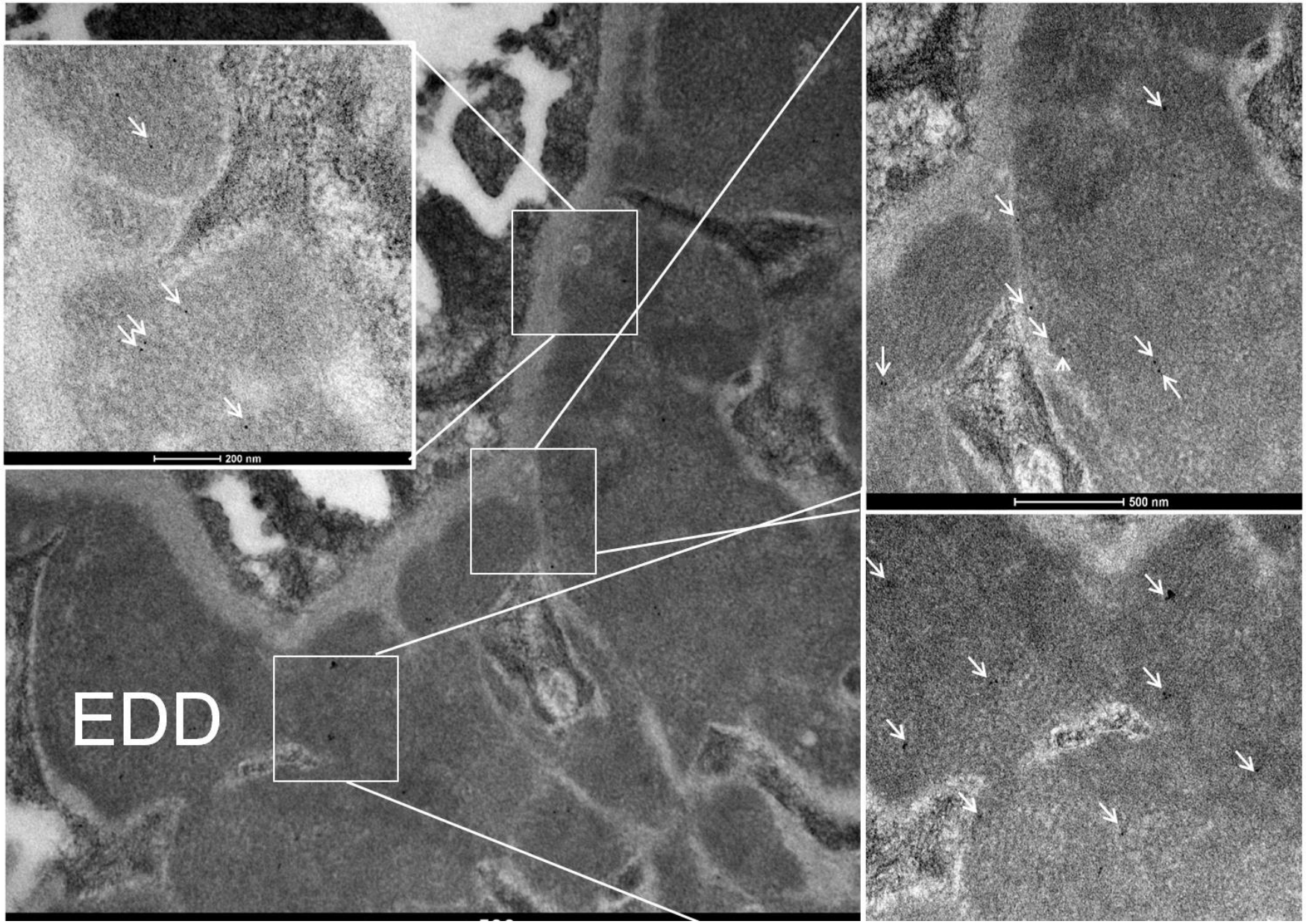

PTX3 is localized inside the EDD. *IEM pictures showing 15 nm gold-labeled PTX3 is indicated inside the EDD (white arrows).*

Footnotes*: PTX3, pentraxin3; EDD: electron dense deposits; IEM, immune-electron microscopy.*

Immunofluorescence

IF was performed to investigate kidney localization of C1q, PTX3, IgG and nuclear antigens in the inflamed kidney and potential differences between the groups. A lupus-like nephritis was confirmed at IIF in most littermates in keeping with the features of the strain, retrieving deposition of IgG antibodies and complement fragments on the GBM and mesangium, yet displaying meaningful differences between PTX3-immunized and non-immunized mice, as described below.

Very interestingly, PTX3 deposits were found mostly in mice not immunized with PTX3 but treated with the sole PBS, indicating that endogenous PTX3 may play a role in the early phases of LN development (F**igure 11)**. Moreover, we observed histones, standing for nuclear material, released in the extracellular space especially in glomeruli of PBS-treated mice, suggesting cell death and chromatin externalization (**Figure 12)**. Notably, PTX3 was shown to colocalize with histones with a good degree of correlation (Pearson's R=0.98; overall range 0.90-0.98) **(Figure 13A and 13B)** while no colocalization was shown with C1q or with IgG (see below), whose deposits were overall remarkably milder in PTX3-immunized mice versus PBS-treated mice (F**igure 14 and Figure 15**).

Figure 11. Glomerular PTX3 deposition in PTX3-immunized vs. PBS-treated age-matched lupus-prone mice

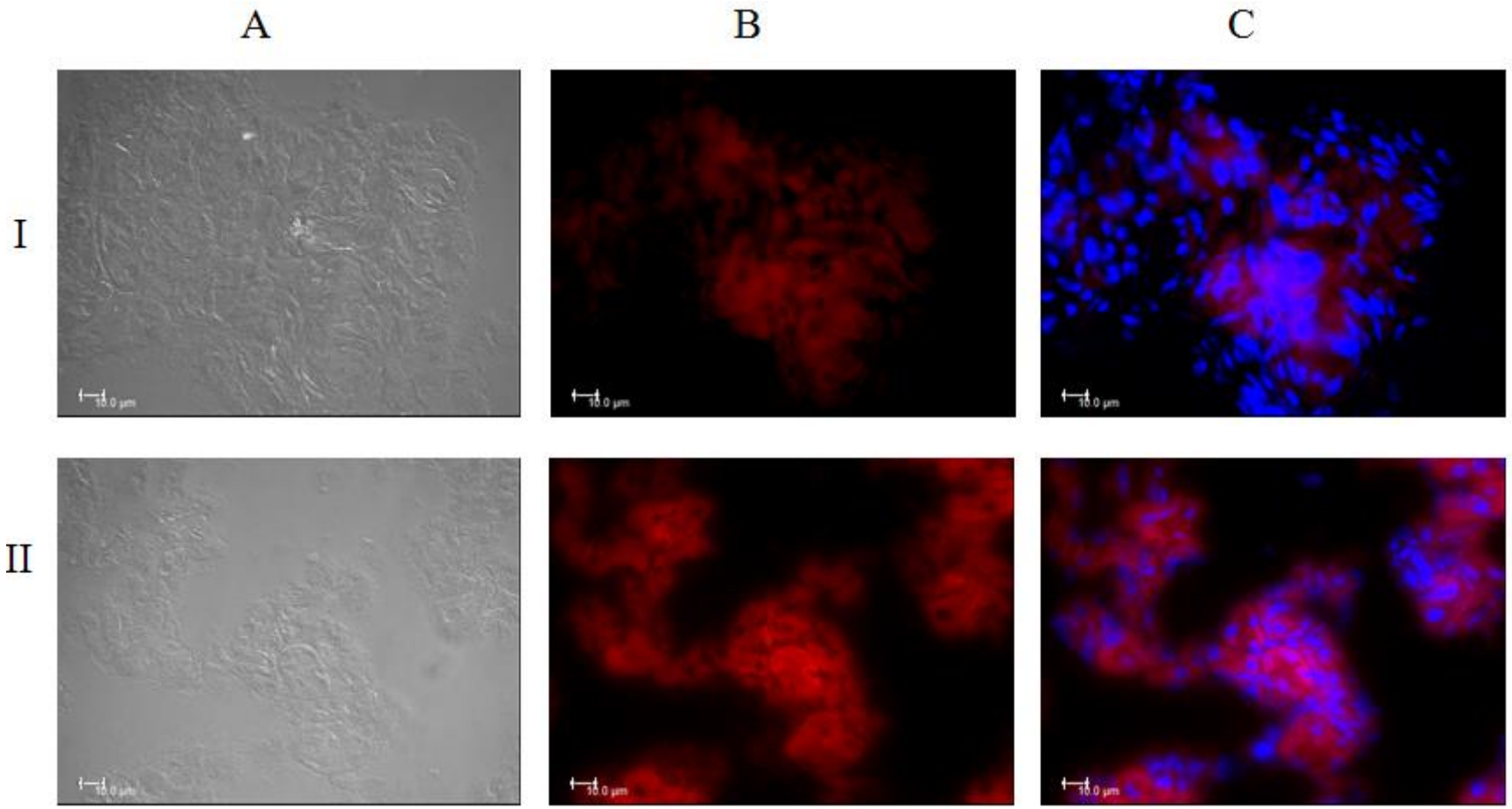

Immunofluorescence imaging of glomerular PTX3 deposition. *Panel I shows a PTX3-immunized mouse and Panel II a PBS-treated mouse, both 22 weeks old. Column A: grey-scale; column B: PTX3 (red fluorescence); column C: merge images. DNA stained with Hoechst (blue fluorescence). PTX3 glomerular deposits are markedly decreased in the PTX3-immunized mouse vs. PBS-treated mouse. Scale bar 10 µm. Magnification: 63x.* ***Footnotes:*** *PTX3, pentraxin3.*

Figure 12. Extracellular deposits of histones in a PTX3-immunized vs. an age-matched PBS-treated mouse

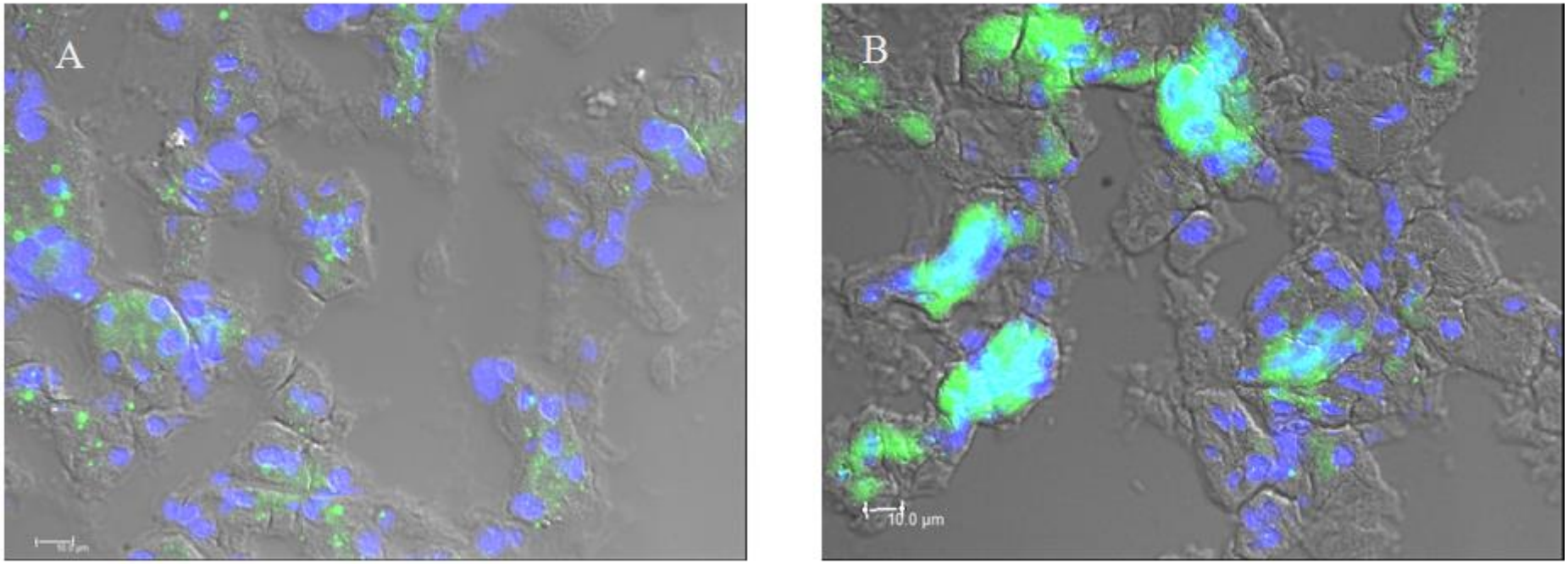

Immunofluorescence showing histones (green fluorescence) leaking out nuclei and localizing in the extracellular space. *(A) Representative picture of a PTX3-immunized mouse; (B) PBS-injected mouse. Background: grey-scale images of renal morphology. DNA stained with Hoechst (blue fluorescence). Scale bar 10 µm. Magnification: 63x.*

Footnotes: *PTX3, pentraxin3, PBS phosphate buffer saline.*

Figure 13. Glomerular PTX3 co-localizes with extracellular histones

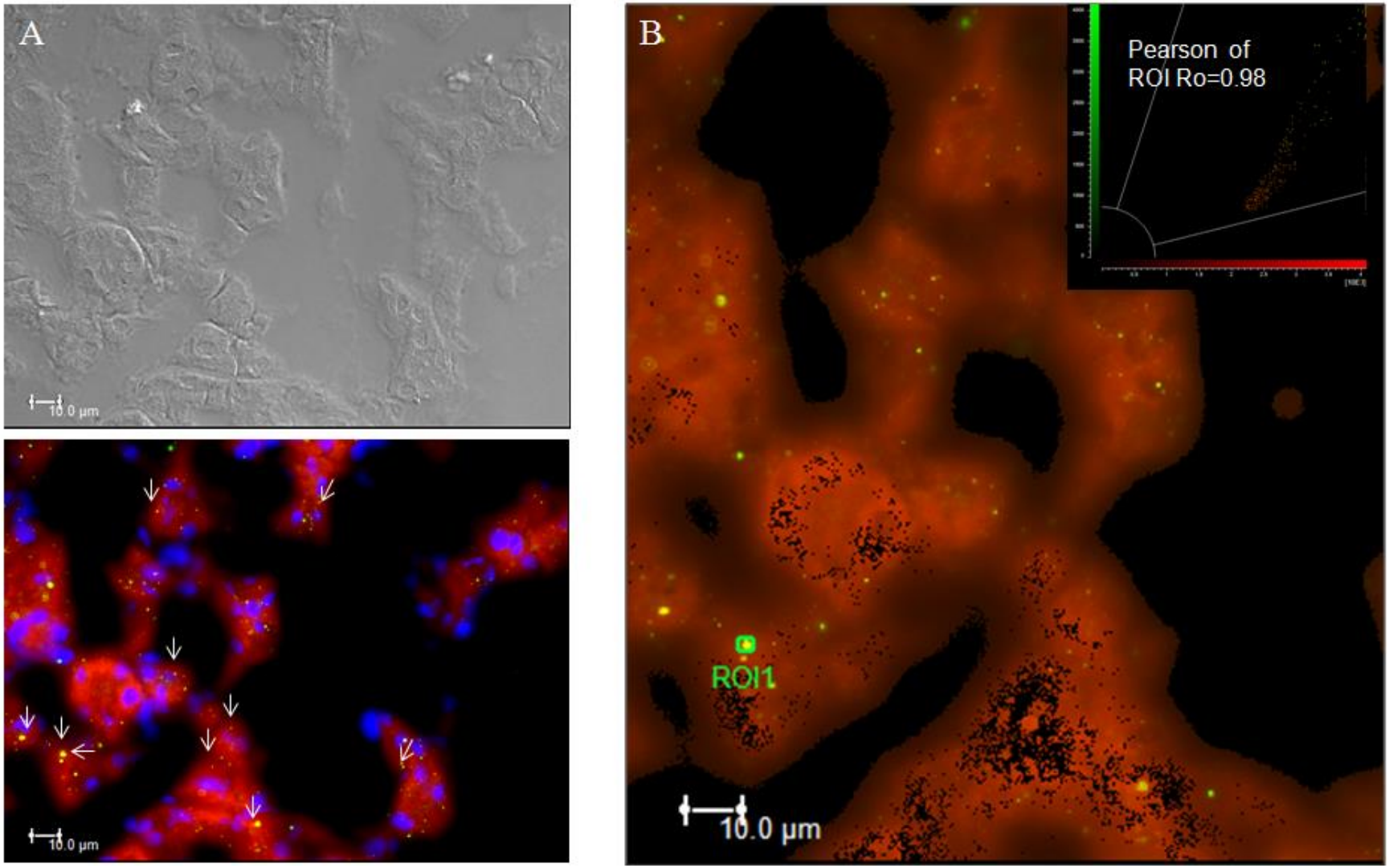

Glomerular PTX3 co-localizes with extracellular histones. (A) *Glomerular morphology is visualized by DIC (grey-scale image). Glomerular deposits of PTX3 (red fluorescence) and extracellular H3 (green) are shown to colocalize at IF (yellow fluorescence and arrows). DNA stained with Hoechst (blue fluorescence). Scale bar 10 µm. Magnification: 63x.* ***(B)*** *Representative immunofluorescence showing colocalization of PTX3 with extracellular histones in one region of interest (ROI, green circle). The yellow fluorescence shows colocalization of PTX3 (red) and histones (green). Colocalization was analysed by Pearson's correlation coefficient (Rr). Significant Pearson's correlation (Rr=0.98) supports true co-localization and not co-expression. Scale bar 10 µm. Magnification: 63x.*

Footnotes: *PTX3, pentraxin3 H3, histone 3; DIC: differential interference contrast; ROI: region of interest*.

Figure 14. Decreased IgG deposits in PTX3-immunized vs. PBS-treated mice

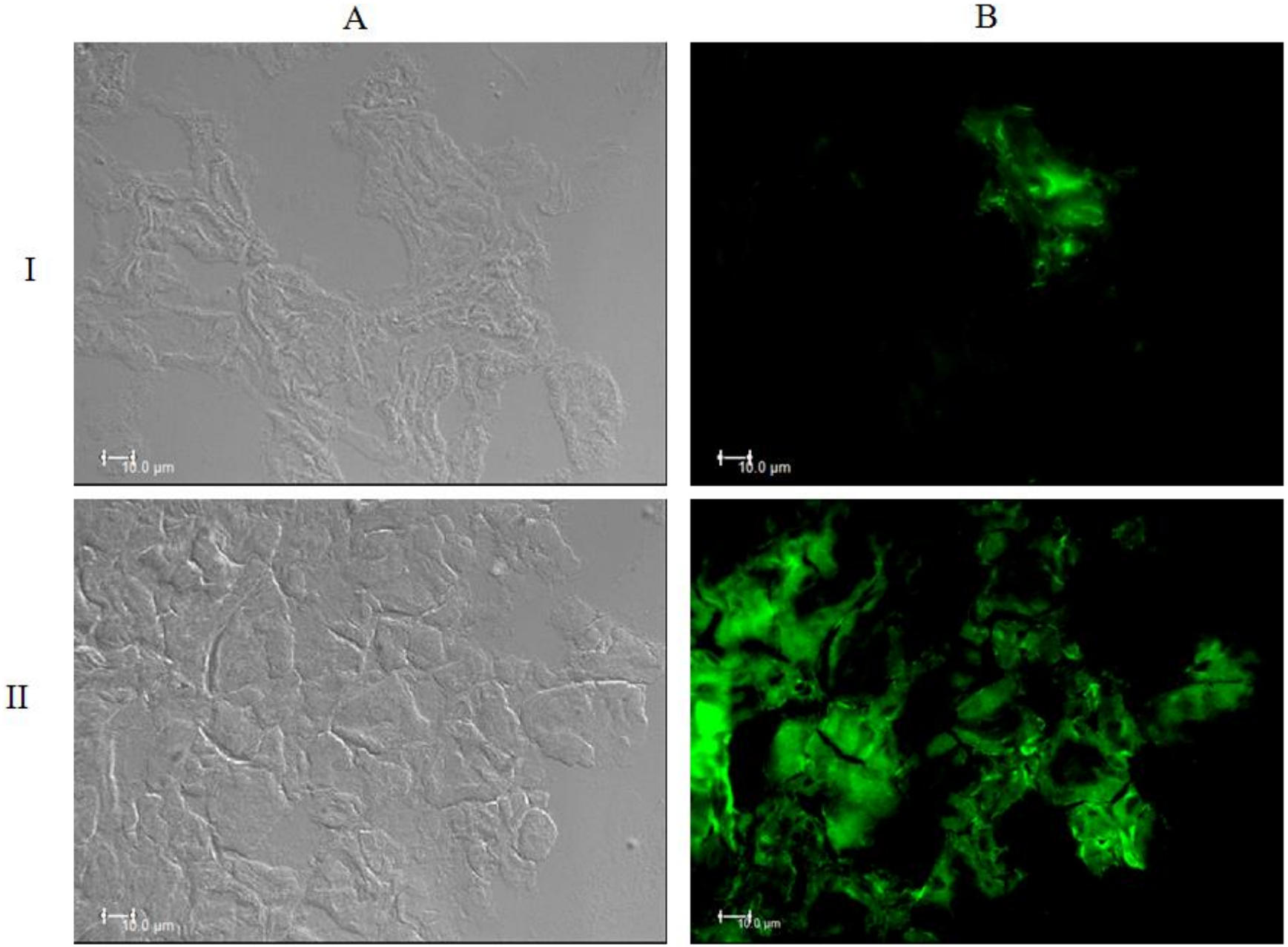

Representative merge images of IgG deposits in one PTX3-immunized and one PBS-treated mouse. *Panel I shows a PTX3-immunized mouse (29 weeks) and panel II a PBS-treated mouse (22 weeks). Column A: grey-scale image; column B: IgG deposits (green fluorescence). IF shows milder signal for IgG deposits in the PTX3-immunized mouse compared to the PBS-treated mouse, consistent with milder renal inflammation. It should be noted that IgG deposition is milder following PTX3 immunization regardless of mice age. Scale bar 10 µm. Magnification: 63x.*

Footnotes*: PTX3, pentraxin3; IgG, immunoglobulin G; IF, immunofluorescence*

Figure 15. Decreased C1q deposits in PTX3-immunized vs. PBS-treated mice

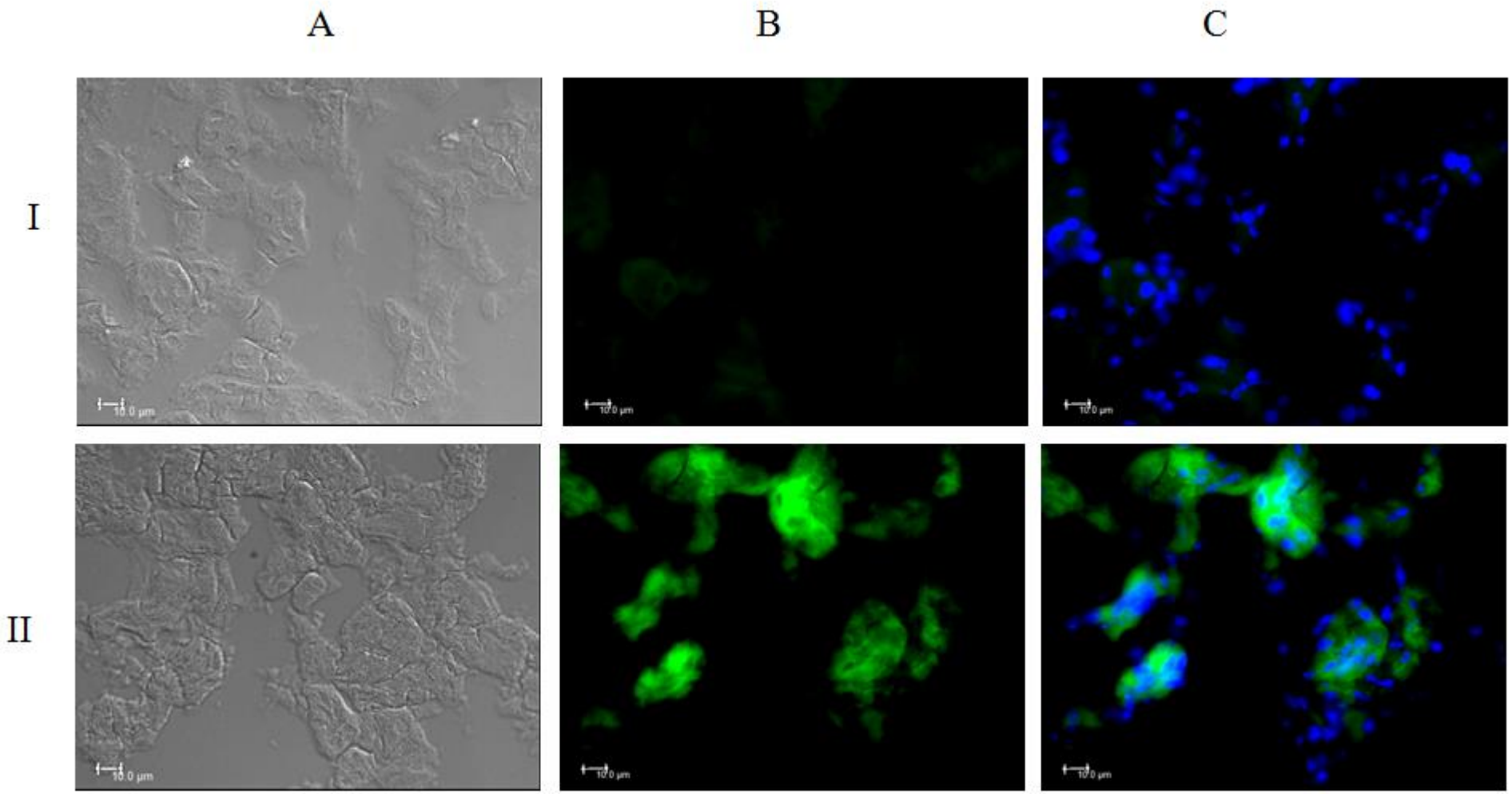

Representative merge images of C1q deposits in one PTX3-immunized and one PBS-treated mouse. *Panel I shows a PTX3-immunized mouse (29 weeks) and panel II a PBS-treated mouse (22 weeks). Column A: grey-scale image; Column B: C1q deposits (green fluorescence); Column C: merged with nuclei (DNA stained with Hoechst, blue). IF shows nearly no signal for C1q deposits in the PTX3-immunized mouse compared to the PBS-treated mouse, consistent with milder renal inflammation. It should be noted that C1q deposition is milder following PTX3 immunization regardless of mice age. Scale bar 10 µm. Magnification: 63x.*

Footnotes*: PTX3, pentraxin3; PBS, phosphate buffer saline; IF, immunofluorescence*

Confocal and light microscopy

Confocal microscopy was performed on renal samples retrieved from the same mice examined at IF, in order to verify IF observations. Thereby, colocalization of PTX3 with histones was confirmed true, as the "z" axis projection provided evidence of PTX3 molecules being present throughout the thickness of the slice and not just optically overlapping. Deposition of IgG, PTX3 and C1q were confirmed milder among PTX3-immunized miceand no relevant colocalization occurred between PTX3, C1q and IgG (**Figure 16**), with the exception of some spot IgG deposits seen only within glomeruli of PTX3-immunized mice that displayed no linear deposition bearing instead a rather patchy distribution, suggesting those were not deposits of nephritogenic anti-chromatin antibodies but rather specific IgG anti-PTX3 antibodies (**Figure 17)**. However, it should be mentioned that PTX3, IgG and C1q molecules are located in close proximity, suggesting co-expression despite no direct binding between to each other.

Unlike ultrastructural abnormalities, histological analysis performed at light microscopy did not reveal major differences among histological lesions in terms of glomerular (percentage of involvement and mesangial hypercellularity) and tubular lesions (dilation and casts) scored as in (112), despite a severe perivascular infiltrate (+4/+5) was slightly more prevalent among PBS-treated mice at 29 weeks (50% vs. 40%). These findings confirm that ultrastructural lesions happen long before optically visible lesions and if not reverted anticipate a subsequent clinically evident nephritis.

Figure 16. Renal PTX3, IgG and C1q deposits are milder in PTX3-immunized mice vs. PBS-treated mice and do not colocalize

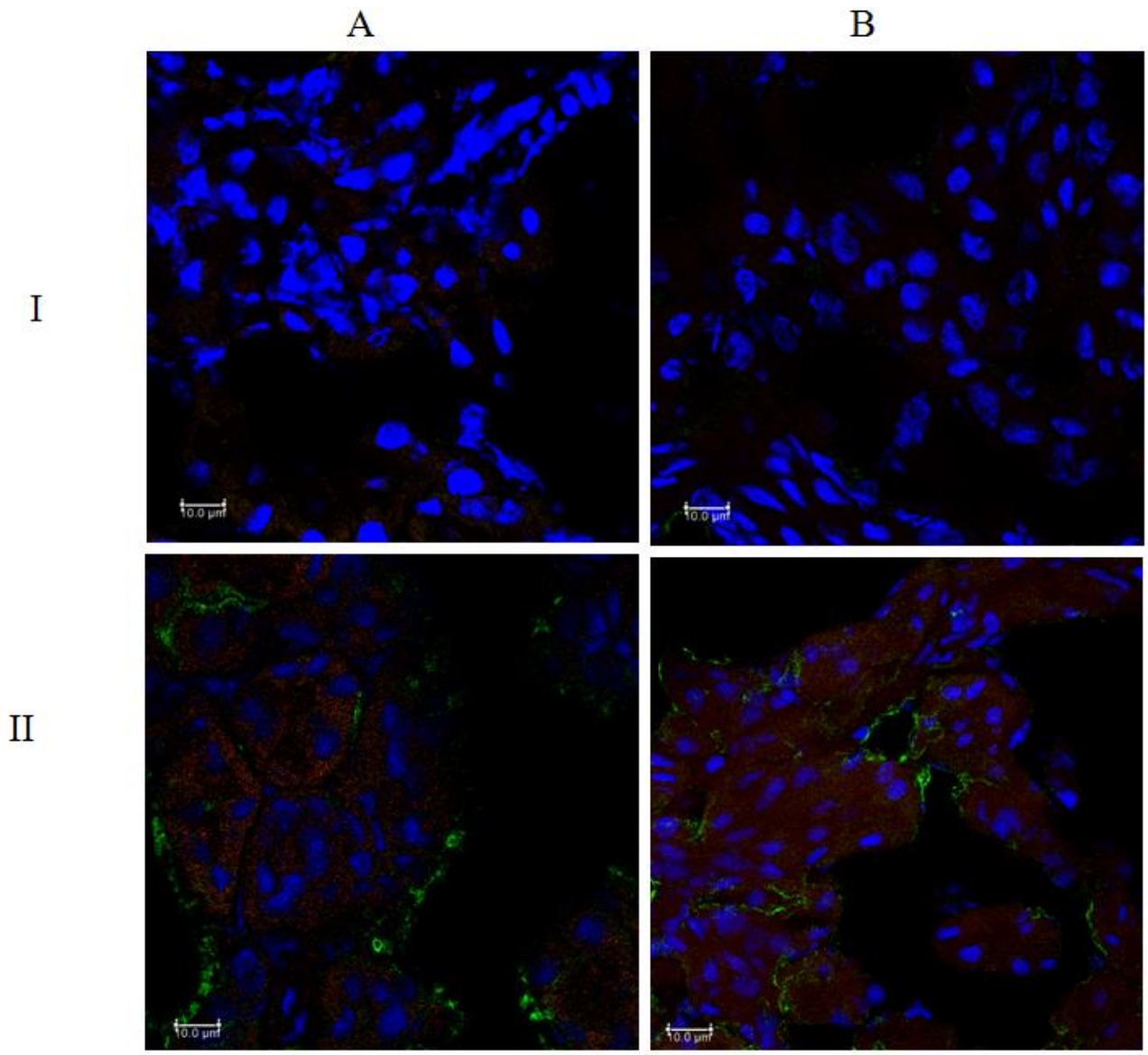

Confocal microscopy showing milder renal PTX3 and IgG deposits in one PTX3-immunized mouse (Panel I) vs. one PBS-treated mouse (Panel II), both aged 22 weeks. *Column A: IgG deposits (green fluorescence) and PTX3 (red); column B: C1q (green) and PTX3 (red). DNA stained with DRAQ5TM (blue). Scale bar 10 µm. Z-interval 1 µm. Zoom factor (Panel II, column B): 2. Magnification: 100x.*

Footnotes*: PTX3, pentraxin3; PBS, phosphate buffer saline.*

Figure 17. IgG deposits in PTX3-immunized and PBS-treated age-matched NZB/W F1 mice

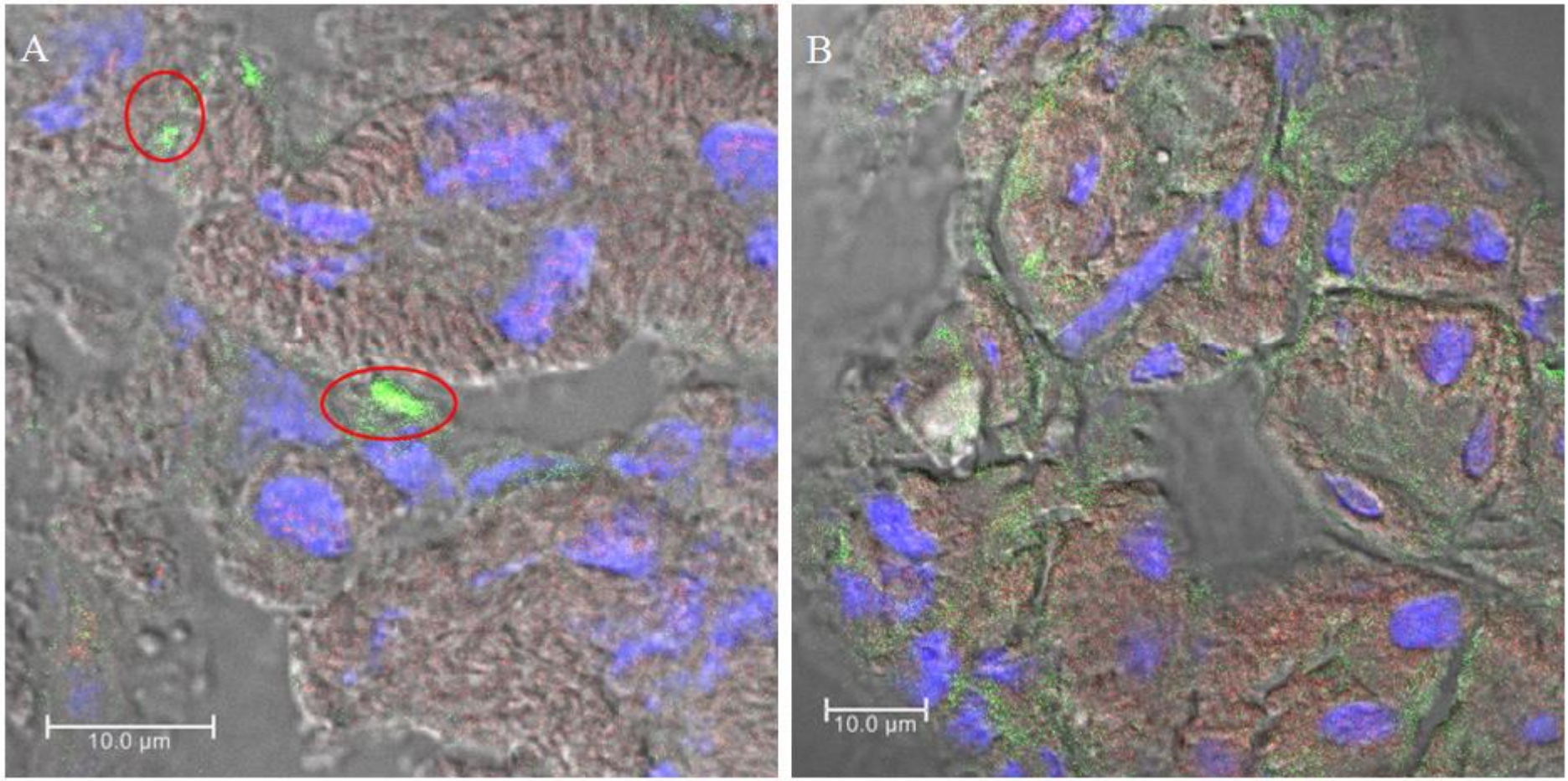

Representative merge images of PTX3 (red fluorescence), IgG deposits (green), nuclei (blue) and DIC (grey scale) in PTX3-immunized and PBS-treated age-matched NZB/W F1 mice. *PTX3-immunized mice (A) show less and spotty IgG deposits compared to wider deposits of both IgG and PTX3 in PBS-immunized mice (B). Yellow fluorescence inside the red circle express colocalization of PTX3 and IgG, suggesting that these may be specific IgG anti-PTX3 antibodies (absent in (B). PTX3 deposits are overall milder in (A). Scale bar 10 µm. Z-interval 1 µm. Magnification: 100x.*

Footnotes*: PTX3, pentraxin3; IgG, immunoglobulin G; New Zealand Black/White F1 mice.*

Flow-cytometry

Flow-cytometry investigating proportion of B cells, Th17 and Treg in spleens and bone marrow did not show significant differences across those populations between the two mice groups. However, it should be noted a trend toward a decreased the Th17/Treg ratio in the spleen of PTX3-immunized mice versus control mice (**Figure 18A),** and an overall decreased Th17/Treg ratio in the bone marrow of PTX3-immunzed versus PBS-treated mice (**Figure 18B**).

Figure 18. Th17/Treg ratio in spleen and BM of PTX3-immunized and PBS-treated mice

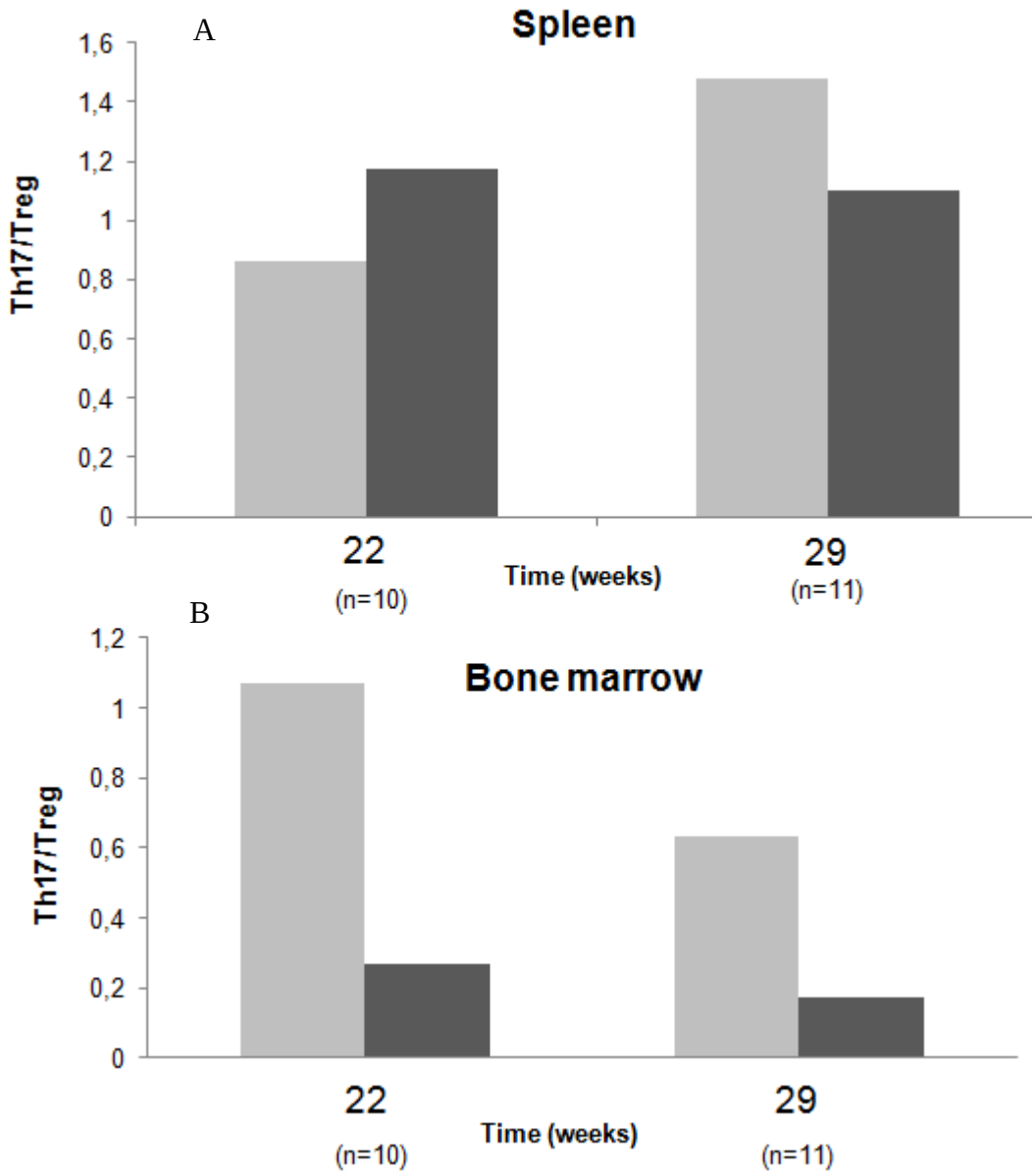

Th17/Treg ratios in spleen and bone marrow of PTX3-immunized vs. PBS-treated mice at sacrifice.

(A) *The ratio is decreased among splenocytes of PTX3-immunized mice despite not reaching statistical significance, and* ***(B)*** *is lower in the BM already at the time of first sacrifice. Mann-Whitney U test.*

Footnotes*: PTX3, pentraxin3; PBS, phosphate buffer saline; BM bone marrow; Th T helper cell; Treg regulatory T cell.*

DISCUSSION

Our observations altogether highlight possible novel pathways of LN development and explore the effects of potential new therapeutic strategies that target those pathways *in vivo*. The use of different lupus-prone strains gave a more complete view on lupus disease as a whole, yet keeping the lupus kidney as the main focus.

During the first year of PhD two parallel studies were carried out (Paper I and II), considering different molecules. First, we postulated that restoration of SERPINB3, whose expression is reduced by high levels of IFNα in SLE (89), would improve the course of the lupus-like disease in two models of lupus-prone mice. Consistent findings, especially regarding the development of a milder lupus-like nephritis following intraperitoneal injections of SERPINB3, suggested that abnormalities linked to the SLE background e.g. the IFN signature may affect different levels of regulation of the immune homeostasis in a really early phase of disease, subsequently resulting in further loss of tolerance. As SERPINB3 is mostly involved in regulation of apoptotic pathways, these observations corroborate the role of apoptotic abnormalities in development of SLE, likely due to aberrant exposition of unremoved debris and uncontrolled enrichment of the autoantigen pool.

On the other hand, the hypothesis chaining subsequent experimental steps resided in PTX3/anti-PTX3 immunity to be an important emerging regulator in development of LN (108-111). Thus, the in vivo evaluation of the clinical effects provided by immunization with hrPTX3 (Paper II) in SLE murine models as well as the characterization of the renal ultrastructural modifications occurring after the immunization (Paper IV, unpublished) represent the mainstays of our work.

In this regard, it should be reminded that development of EDD in the lupus kidney was associated with impending renal inflammation since a long time (119) and was experimentally proven in diverse autoimmune strains (12,44). EDD in mice consist of not-removed nuclear material including histones and chromatin and trapped antibodies, suggesting that they would act as an initiating platform on which anti-chromatin antibodies could deposit to foster renal inflammation (14,15).

Indeed, nephritogenic anti-chromatin autoantibodies in LN murine models were shown to initially accumulate in mesangial EDD, while showing no cross-reactivity with native GBM epitopes (51), thereby suggesting that EDD retain the relevant antigens for renal inflammation and confer a selective harmful potential to anti-chromatin antibodies when gathered together with their target antigens.

Using different technologies, we documented on the one hand that mesangial and membrane-associated EDD are abundant already at very early stages of disease in mice developing a lupus-like nephritis, yet on the other hand we showed that their formation can be hindered through a specific antigen-driven treatment. Moreover, IEM observations in our study indicate that PTX3 does colocalize with nuclear material and that the colocalization happens mostly inside the EDD in the GBM or in the mesangium, suggesting that PTX3 is indeed a native component of the EDD. In fact, most PTX3 deposits were found in lupus-prone mice not immunized with hrPTX3, meaning that they could not be attributed to a passive injection of the antigen, being rather a naturally occurring event during LN development.

Interestingly, C-reactive protein (CRP) which belongs to the short-pentraxins and whose specificity was previously retrieved among SLE autoantibodies, was recently identified inside the EDD in lupus patients (120), suggesting EDD may have a more heterogeneous composition than previously thought.

Our data so far allow to pinpoint a pre- and post-treatment landscape comparing control mice with PTX3-immunized mice. In fact, PTX3-immunized mice display nearly no EDD or podocyte effacement compared to control littermates (**Figure 9**); moreover, PTX3-immunized mice show a remarkable decrease in glomerular IgG and C1q deposits as well as in PTX3 expression (**Figures 11, 14, 15, 16**), suggesting that an acquired immunity against PTX3 is effective in hindering the progression of the renal inflammatory process from the preclinical to more advanced stages (**Figure 19**). In this regard, absence of profound differences at optical microscopy between the PTX3 and

PBS groups may be consistent with a lag time required for the transition from a silent to a proliferative nephritis, which is anticipated by flourishing ultrastructural abnormalities.

Assuming EDD as a founding spot in LN development, it is tempting to speculate that autoantigens retained in EDD play a role in LN course. The link between autoantigen exposure and specific autoantibody production is highly presumable, although still not demonstrated for anti-nuclear antibodies. According to current knowledge, aberrant exposure of nuclear acids linked to nuclear proteins could, if not ignite, at least sustain an anti-nuclear antibody response via stimulation of T helper cells (14), which may be also hypothesized for other antigens aberrantly exposed in density centers like the EDD.

Interestingly, previous findings by us and others have suggested that anti-PTX3 antibodies may be protective against LN development, as their presence is nearly confined to SLE patients not developing LN (108-110). In order to check whether this was a mere association or anti-PTX3 antibodies truly exerted a protective effect against LN, we immunized lupus-prone mice with hrPTX3 and compared them with control littermates immunized with PBS, investigating clinical and serological features (Paper II). We could show that only mice immunized with PTX3 developed anti-PTX3 antibodies and that these mice lived significantly longer and healthier than their matched controls, remarkably displaying a milder lupus-like nephritis as they developed anti-dsDNA, anti-C1q antibodies and proteinuria significantly later and at significantly lower levels in respect to control mice. These observations therefore point to a true anti-nephritic effect of anti-PTX3 antibodies *in vivo,* whose production might be triggered by aberrant exposition of PTX3 in EDD. Hence, PTX3 may be considered as a novel key antigen involved in the initial development of lupus-like nephritis.

The reason why anti-PTX3 autoantibodies could be protective was investigated starting from previous observations on PTX3-C1q interaction, as it was shown that in presence of abundant apoptotic debris PTX3 may bind to early apoptotic bodies and function as a platform for C1q to be fixed and activated (99,104). Hence, the finding that a relevant rate of anti-PTX3 antibodies from

lupus patients belonged to the IgG4 pool (Paper II) suggests that they intrinsically entail a poor complement-activating potential, although IC formation is barely affected *in vitro*.

Overall, most anti-PTX3 antibodies belong to the IgG subclass just like anti-chromatin antibodies, suggesting an upstream antigen-driven response heralding their generation. However, a B cell receptor specific forPTX3 was not characterized so far which links PTX3 binding to B cells in a classical receptor-antigen fashion. In our experiments, we attempted at identifying any PTX3-specific circulating B cell in peripheral blood of SLE patients with or without LN and healthy controls, in order to investigate whether these cells do exist, although in small amount in the bloodstream, and whether they follow a different distribution among LN and non-LN lupus patients (Paper III). Our results have shown that a small population of circulating $CD19^+$ cells exists which can bind PTX3 with a reasonable degree of specificity (Paper III). Interestingly, regardless of the treatment and of disease activity, LN patients displayed the lowest amount of both absolute number and proportion of circulating PTX3-B cells if compared with non-LN patients and HD, who instead looked broadly alike either in terms of specific B cell amount and subsets distribution. In fact, most circulating PTX3-B cells in those groups belonged to naïve $CD20^+CD27^-IgD^+$ subset, while the second most frequent were pre-switched $CD20^+CD27^+IgD^+$, followed by switched memory B cells $CD20^+CD27^+IgD^-$, whereas LN patients displayed nearly no $CD20^+$ PTX3-B cells.

Two main questions would arise from such findings, e.g. what is the real function of circulating PTX3-specific B cells and why non-renal SLE are more similar to HD than to LN patients, provided that blood was withdrawn before any initial therapy for LN was performed. So far, no certain data can answer these questions, however it is tempting to speculate that the bulk of mature naïve PTX3-B cells could represent an early B cell pool heralding development of a PTX3-specific B cell response as part of a natural immunity, which then evolves into a more structured adaptive response with autoantibody production only in SLE patients but not in HD. Alternatively and not mutually exclusively, the abundance of naïve $PTX3^+$ B cells in non renal SLE may represent a reaction of

polyreactive B cells, which is a common feature of SLE (121), giving rise to antibody secreting cells *via* an extrafollicular pathway (122), consistently with the progressive decrease in $PTX3^+$B cell subsets from naïve to switched-memory cells.

Furthermore, the second most prominent PTX3-B cell population consisted of $CD20^+CD27^+IgD^+$ B cells, which were described to display half-way features between MZ and non-switched memory B cells (123,124). Because IgG anti-PTX3 antibodies are significantly more prevalent among SLE patients, it may be hypothesized that at least a proportion of $PTX3^+CD27^+IgD^+$ cells bear a true memory phenotype, entailing the chance of further switching and differentiation into antibody secreting cells (125).

In other words, it is possible that the viewpoint offered by peripheral blood of unselected SLE patients and HD reflects a steady-state situation of a natural immunity against PTX3, which may play an immunomodulatory function in case of disease reactivation. This level of anti-PTX3 self control could be prematurely lost or never arise in SLE patients who are then committed to develop LN.

In summary, our work highlighted three novel points in LN development: i) abnormalities in the expression or function of physiologically ubiquitous molecules, even though not tightly related to the immune response e.g. SERPINB3, occur in the preclinical phase of SLE and may subsequently impact on development of LN, in an unpredictable fashion; ii) PTX3 is a novel key antigen in LN; iii) the development of a PTX3-directed immunity is selectively protecting against LN development (**Figure 19**). These observations are relevant in a short and long term perspective, as validation of anti-PTX3 antibody prevalence and inverse correlation with LN could pave the way to their dosage as a tool for patient stratification, while stimulating further development of therapies directed against aberrantly expressed self antigens in the therapy of SLE and other autoimmune rheumatic systemic diseases.

Figure 19 ©. Proposed models and role of PTX3-anti-PTX3 immunity in development of LN

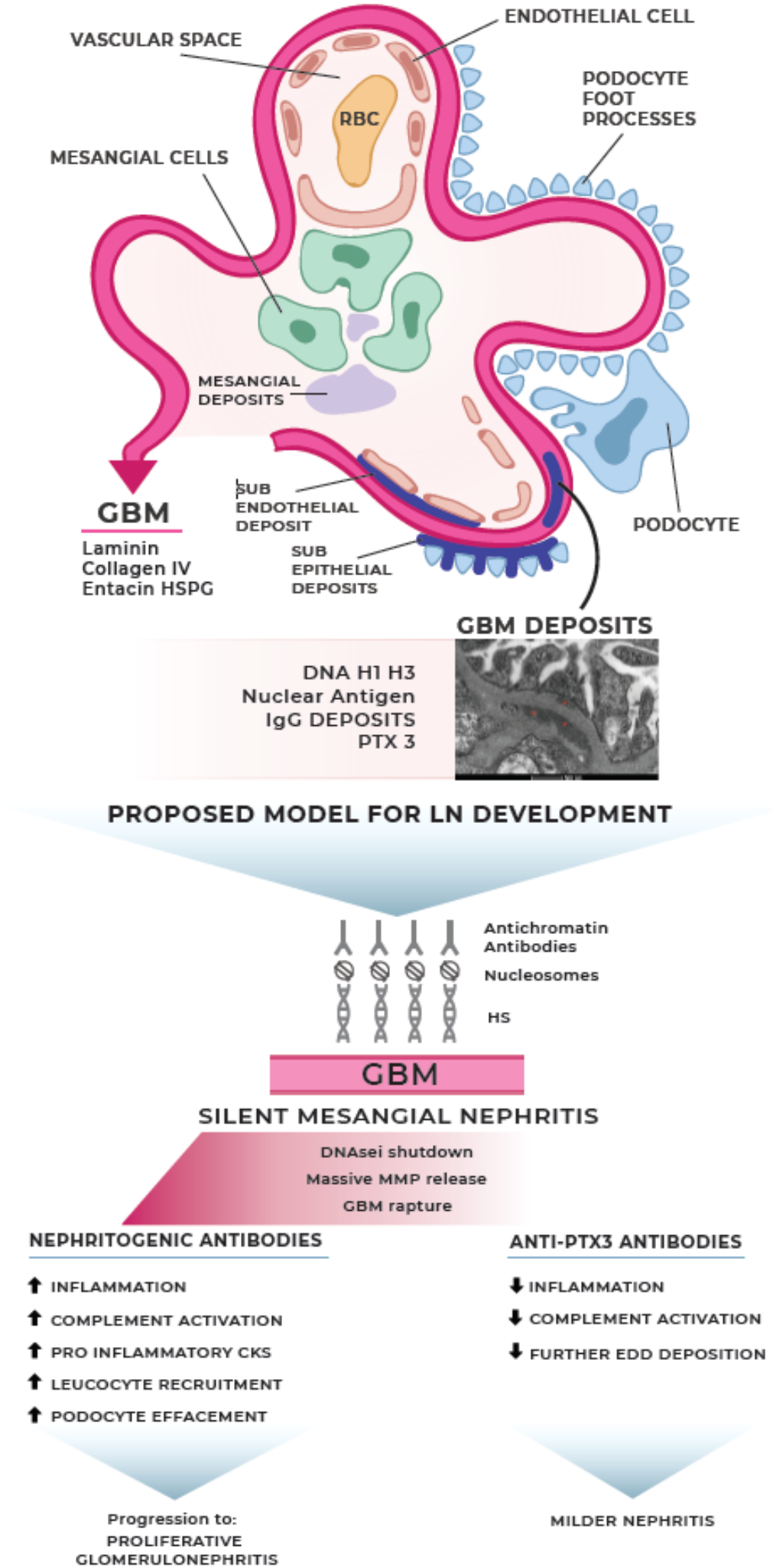

Proposed models and role of PTX3-anti-PTX3 immunity in development of LN. *The currently accepted model for development of LN (15) envisions the binding of anti-chromatin antibodies to nucleosomes aberrantly exposed in the EDD (containing chromatin, IgG and PTX3) and establishment of a silent mesangial LN. At this stage, mesangial cells still exert a scavenging effect with IC removal. The transition from a silent LN to a proliferative and clinically evident LN is supported by a shutdown in DNAse I expression and a rapid accumulation of large chromatin fragments, IC and inflammatory mediators, resulting in both a IC-mediated inflammation and innate-mediated release of MMP and inflammatory cytokines with progressive damage of the GBM and/or of the podocyte processes, in a self-sustaining loop. In this scenario, we hypothesize that anti-PTX3 antibodies may prevent renal PTX3 deposition exerting an overall anti-inflammatory effect eventually resulting in a decreased formation of EDD which in turn could dampen the pro-inflammatory interaction of nephritogenic antibodies with abnormally exposed nuclear antigens, thus counteracting the transition from a silent mesangial to an overt LN.*

Footnotes*: EDD, electron dense deposits; LN, lupus nephritis; PTX3, pentraxin3; GBM glomerular basement membrane; IC, immune-complexes; MMP, metalloproteinase.*

References

1 Doria A, Iaccarino L, Ghirardello A, Zampieri S, Arienti S, Sarzi-Puttini P, Atzeni F, Piccoli A, Todesco S. Long-term prognosis and causes of death in systemic lupus erythematosus. Am J Med 2006;119:700-6

2 Almaani S, Meara A, Rovin BH. Update on Lupus Nephritis. Clin J Am Soc Nephrol 2017;12:825-835.

3 Dooley MA, Jayne D, Ginzler EM, Isenberg D, Olsen NJ, Wofsy D, Eitner F, Appel GB, Contreras G, Lisk L, Solomons N; ALMS Group Mycophenolate versus azathioprine as maintenance therapy for lupus nephritis. N Engl J Med 2011;365:1886–1895

4 Contreras G, Pardo V, Cely C, Borja E, Hurtado A, De La Cuesta C, et al. Factors associated with poor outcomes in patients with lupus nephritis. Lupus 2005;14: 890–895.

5 Tektonidou M, Dasgupta A, Ward M: Risk of end-stage renal disease in patients with lupus nephritis, 1970-2015: A systematic review and Bayesian meta-analysis. Arthritis Rheumatol 2016;68:1432–1441.

6 Bajema IM, Wilhelmus S, Alpers CE, Bruijn JA, Colvin RB, Cook HT, et al. Revision of the International Society of Nephrology/Renal Pathology Society classification for lupus nephritis: clarification of definitions, and modified National Institutes of Health activity and chronicity indices. Kidney Int 2018;93:789-796.

7 Yu F, Haas M, Glassock R, Zhao MH. Redefining lupus nephritis: clinical implications of pathophysiologic subtypes. Nat Rev Nephrol 2017;13:483-495.

8 Davidson A. What is damaging the kidney in lupus nephritis. Nat Rev Rheumatol 2016; 12:143-53.

9 Tsokos G, Buyon JP, Koike T, Lahita G, editors. The pathology of lupus nephritis. In: Systemic lupus erythematosus, 5th ed. Elsevier, 2016 . Pp 351-69

10 Rekvig OP, Thiyagarajan D, Pedersen HL, Horvei KD, Seredkina N. Future Perspectives on Pathogenesis of Lupus Nephritis: Facts, Problems, and Potential Causal Therapy Modalities. Am J Pathol 2016;186:2772-2782.

11 Seredkina N, Van Der Vlag J, Berden J, Mortensen E, Rekvig OP. Lupus nephritis: enigmas, conflicting models and an emerging concept. Mol Med 2013;19:161-9.

12 Horvei KD, Pedersen HL, Fismen S, Thiyagarajan D, Schneider A, Rekvig OP, et al. Lupus nephritis progression in FcγRIIB-/-yaa mice is associated with early development of glomerular electron dense deposits and loss of renal DNase I in severe disease. PLoS ONE 2017;12:e0188863.

13 Gatto M, Iaccarino L, Ghirardello A, Punzi L, Doria A. Clinical and pathologic considerations of the qualitative and quantitative aspects of lupus nephritogenic autoantibodies: A comprehensive review. J Autoimmun 2016;69:1-11.

14 Rekvig OP. The dsDNA,Anti-dsDNA Antibody, and LupusNephritis: What We Agree on, WhatMust Be Done, and What the Best Strategy Forward Could Be. Front. Immunol 2019;10:1104.

15 Rekvig OP, Putterman C, Casu C, Gao HX, Ghirardello A, Mortensen ES, Tincani A, Doria A. Autoantibodies in lupus: culprits or passive bystanders? Autoimmun Rev 2012;11:596-603.

16 Thanei S, Vanhecke D, Trendelenburg M. Anti-C1q autoantibodies from systemic lupus erythematosus patients activate the complement system via both the classical and lectin pathways. Clin Immunol 2015;160:180-7

17 Pérez de Lema G, Maier H, Nieto E, et al. Chemokine expression precedes inflammatory cell infiltration and chemokine receptor and cytokine expression during the initiation of murine lupus nephritis. J Am Soc Nephrol 2001;12:1369-82

18 Duffield JS. Macrophages in kidney repair and regeneration. J Am Soc Nephrol 2011;22:199–201.

19 Villanueva E, Yalavarthi S, Berthier CC, Hodgin JB, Khandpur R, Lin AM, Rubin CJ, Zhao W, Olsen SH, Klinker M, Shealy D, Denny MF, Plumas J, Chaperot L, Kretzler M, Bruce AT, Kaplan

MJ. Netting neutrophils induce endothelial damage, infiltrate tissues, and expose immunostimulatory molecules in systemic lupus erythematosus. J Immunol 2011;187:538-52.

20 Wither JE, Prokopec SD, Noamani B, et al. Identification of a neutrophil- related gene expression signature that is enriched in adult systemic lupus erythematosus patients with active nephritis: clinical/pathologic associations and etiologic mechanisms. Plos One 2018;13:e0196117.

21 Toro-Domínguez D, Martorell-Marugán J, Goldman D, et al. Stratification of Systemic Lupus Erythematosus Patients Into Three Groups of Disease Activity Progression According to Longitudinal Gene Expression. Arthritis Rheumatol 2018;70:2025-2035

22 Schrimpf C, Teebken OE, Wilhelmi M, Duffield JS. The role of pericyte detachment in vascular rarefaction. J Vasc Res 2014;51:247–258.

23 Moroni G, Quaglini S, Radice A, Trezzi B, Raffiotta F, Messa P, et al., The value of a panel of autoantibodies for predicting the activity of lupus nephritis at time of renal biopsy, J Immunol Res 2015 (2015) 106904.

24 Mok CC, Ho L, Leung HW, Wong LG. Performance of anti-C1q, antinucleosome, and anti-dsDNA antibodies for detecting concurrent disease activity of systemic lupus erythematosus. Transl Res 2010;156:320e325

25 Rock KL, Benacerraf B, Abbas AK. Antigen presentation by hapten-specific B lymphocytes. J Exp Med 1984;160:1102-1113.

26 Munoz LE, Lauber K, Schiller M, Manfredi AA, Herrmann M. The role of defective clearance of apoptotic cells in systemic autoimmunity. Nat Rev Rheumatol 2010;6:280-289.

27 Van Ghelue M, Moens U, Bendiksen S, Rekvig OP. Autoimmunity to nucleosomes related to viral infection: a focus on hapten-carrier complex formation. J Autoimmun 2003;20:171-182.

28 Andreassen K, Moens U, Nossent H, Marion TN, Rekvig OP. Termination of human T cell tolerance to histones by presentation of histones and polyomavirus T antigen provided that T antigen is complexed with nucleosomes, Arthritis Rheum 1999;42:2449-2460.

29 Radic M, Herrmann M, van der Vlag J, Rekvig OP, Regulatory and pathogenic mechanisms of autoantibodies in SLE. Autoimmunity 2011;44:349-356.

30 Andreassen K, Bendiksen S, Kjeldsen E, Van Ghelue M, Moens U, Arnesen E, et al. T cell autoimmunity to histones and nucleosomes is a latent property of the normal immune system. Arthritis Rheum 2002;46:1270-1281.

31 Desai DD, Krishnan MR, Swindle JT, Marion TN. Antigen-specific induction of antibodies against native mammalian DNA in nonautoimmune mice. J Immunol 1993;151:1614-26.

32 Aas-Hanssen K, Funderud A, Thompson KM, Bogen B, Munthe LA. Idiotype-specific Th cells support oligoclonal expansion of anti-dsDNA B cells in mice with lupus. J Immunol 2014;193: 2391-2398.

33 Munthe LA, Kyte JA, Bogen B. Resting small B cells present endogenous immunoglobulin variable-region determinants to idiotype specific CD4þ T cells in vivo. Eur J Immunol 1999;29: 4043-4052.

34. Jacobsen JT, Lunde E, Sundovold-Gjerstad V, Munthe LA, Bogen B. The cellular mechanism by which complementary Idþ and anti-Id antibodies communicate: T cells integrated into idiotypic regulation Immunol Cell Biol 2010;88:515-522.

35 Munthe LA, Os A, Zangani M, Bogen B. MHC-restricted Ig V region-driven T-B lymphocyte collaboration: B cell receptor ligation facilitates switch to IgG production. J Immunol 2004;172:7476-7484

36 Snyder CM, Aviszus K, Heiser RA, Tonkin DR, Guth AM, Wysocki LJ. Activation and tolerance in CD4(þ) T cells reactive to an immunoglobulin variable region. J Exp Med 2004;200:1-11.

37 Munthe LA, Corthay A,Os A, Zangani M, Bogen B. Systemic autoimmune disease caused by autoreactive B cells that receive chronic help from Ig V region-specific T cells. J Immunol 2005;175:2391-2400.

38 Aas-Hanssen K, Thompson KM, Bogen B, Munthe LA. Systemic lupus erythematosus: molecular mimicry between anti-dsDNA CDR3 idiotype, microbial and self peptideseas antigen for Th cells. Front Immunol 2015;6.

39 Yung S, Chan TM. Mechanisms of kidney injury in lupus nephritisethe role of Anti-dsDNA antibodies. Front Immunol 2015;6:475

40 Edgington SM, Stollar BC. Immunogenicity of Z-DNA depends on the size of polynucleotide presented in complexes with methylated BSA. Mol Immunol 1992;29:609-617.

41 Radic M, Marion T, Monestier M. Nucleosomes are exposed at the cells surface in apoptosis. J Immunol 2004;172:6692-6700.

42 Nielsen T, Østergaard O, Stener L, Iversen LV, Truedsson L, Gullstrand B, et al. Increased IgG on cell-derived plasma microparticles in systemic lupus erythematosus is associated with autoantibodies and complement activation. Arthritis Rheum 2012;64:1227-1236.

43 Mehra S, Fritzler MJ. The spectrum of anti-chromatin/nucleosome autoantibodies: independent and interdependent biomarkers of disease. J Immunol Res 2014;368274.

44 Kalaaji M, Fenton KA, Mortensen ES, Olsen R, Sturfelt G, Alm P, et al.Glomerular apoptotic nucleosomes are central target structures for nephritogenic antibodies in human SLE nephritis. Kidney Int 2007;71:664-672.

45 Mortensen ES, Rekvig OP. Nephritogenic potential of anti-DNA antibodies against necrotic nucleosomes. J Am Soc Nephrol 2009;20:696-704.

46 Kalaaji M, Mortensen E, Jørgensen L, Olsen R, Rekvig OP. Nephritogenic lupus antibodies recognize glomerular basement membrane-associated chromatin fragments released from apoptotic intraglomerular cells. Am J Pathol 2006;168:1779-1792.

47 Mjelle JE, Rekvig OP, Fenton KA. Nucleosomes possess a high affinity for glomerular laminin and collagen IV and bind nephritogenic antibodies in murine lupus-like nephritis. Ann Rheum Dis 2007; 66:1661-1668.

48 Li T, Prokopec SD, Morrison S, et al. Anti-nucleosome antibodies outperform traditional biomarkers as longitudinal indicators of disease activity in systemic lupus erythematosus. Rheumatology (Oxford) 2015;54:449-57

49 Ghirardello A, Doria A, Zampieri S, Tarricone E, Tozzoli R, Villalta D, et al., Antinucleosome antibodies in SLE: a two-year follow-up study of 101 patients. J Autoimmun 2004;22:235-240.

50 Muller S, Dieker J, Tincani A, Meroni PL. Pathogenic anti-nucleosome antibodies. Lupus 2008;17:431-436.

51 van Bavel CC, Fenton KA, Rekvig OP, van der Vlag J, Berden JH. Glomerular targets of nephritogenic autoantibodies in systemic lupus erythematosus. Arthritis Rheum 2008;58:1892-1899.

52 Mostoslavsky G, Fischel R, Yachimovich N, Yarkoni Y, Rosenmann E, Monestier M, et al. Lupus anti-DNA autoantibodies cross-react with a glomerular structural protein: a case for tissue injury by molecular mimicry. Eur J Immunol 2001;31:1221-1227.

53 Krishnan MR,Wang C, Marion TN. Anti-DNA autoantibodies initiate experimental lupus nephritis by binding directly to the glomerular basement membrane in mice. Kidney Int 2012; 82:184-192.

54 Deocharan B, Qing X, Lichauco J, Putterman C. Alpha-actinin is a crossreactive renal target for pathogenic anti-DNA antibodies. J Immunol 2002;168:3072-3078.

55 Deocharan B, Zhou Z, Antar K, Siconolfi-Baez L, Angeletti RH, Hardin J, et al. Alpha-actinin immunization elicits anti-chromatin autoimmunity in non autoimmune mice. J Immunol 2007;179: 1313-1321.

56 Becker-Merok A, Kalaaji M, Haugbro K, Nikolaisen C, Nilsen K, Rekvig OP, et al. Alpha-actinin-binding antibodies in relation to systemic lupus erythematosus and lupus nephritis. Arthritis Res Ther 2006;8:R162.

57Kalaaji M, Sturfelt G, Mjelle JE, Nossent H, Rekvig OP. Critical comparative analyses of anti-alpha-actinin and glomerulus-bound antibodies in human and murine lupus nephritis. Arthritis Rheum 2006;54:914-926

58 Manson JJ, Ma A, Rogers P, Mason LJ, Berden JH, van der Vlag J, et al., Relationship between anti-dsDNA ,anti-nucleosome and anti-alpha-actinin antibodies and markers of renal disease in patients with lupus nephritis:a prospective longitudinal study. Arthritis Res Ther 2009;11:R154.

59 Iaccarino L, Ghirardello A, Canova M, Zen M, Bettio S, Nalotto L, Punzi L, Doria A. Anti-annexins autoantibodies: Their role as biomarkers of autoimmune diseases. Autoimmun Rev 2011;10 :553-558.

60 Caster DJ, Korte EA, Merchant ML, Klein JB, Wilkey DV, Rovin BH, et al., Autoantibodies targeting glomerular annexin A2 identify patients with proliferative lupus nephritis. Proteomics Clin Appl 2015;9:1012-20.

61 Yung S, Cheung K, Zhang Q, Chan TM. Anti-dsDNA antibodies bind to mesangial annexin II in lupus nephritis. J Am Soc Nephrol 2010;21:1912-1927.

62 Alarcon-Segovia D. Antinuclear antibodies: to penetrate or not to penetrate that was the question. Lupus 2001;10:315-318.

63 Hanrotel-Saliou C, Segalen I, Le Meur Y, Youinou P, Renaudineau Y. Glomerular Antibodies in Lupus Nephritis Clin Rev Allerg Immunol 2011;40:151-158.

64. Bruijn JA, van Leer EH,. Baelde HJ, Corver WE, Hogendoorn PC, Fleuren GJ. Characterization and in vivo transfer of nephritogenic autoantibodies directed against dipeptidyl peptidase IV and laminin in experimental lupus nephritis. Lab Invest 1990;63:350-359.

65 Dieker JW, Sun YJ, Jacobs CW, Putterman C, Monestier M, Muller S, van der Vlag J, Berden JH. Mimotopes for lupus-derived anti-DNA and nucleosome-specific autoantibodies selected from random peptide phage display libraries: facts and follies. J Immunol Methods 2005;296:83-93.

66. van Bruggen MC, Walgreen B, Rijke TP, Tamboer W, Kramers K, Smeenk RJ, Monestier M, Fournie GJ, Berden JH. Antigen specificity of anti-nuclear antibodies complexed to nucleosomes determines glomerular basement membrane binding in vivo. Eur J Immunol 1997;27:1564-9.

67 Mjelle JE, Rekvig OP, Van Der Vlag J, Fenton KA. Nephritogenic antibodies bind in glomeruli through interaction with exposed chromatin fragments and not with renal cross-reactive antigens. Autoimmunity 2011;44:373-83.

68 Zykova SN, Serekdina NE, Rekvig OP. Glomerular targets for autoantibodies in lupus nephritis: an apoptotic origin. Ann NY Acad Sci 2007;1108:1-10.

69 Pickering MC, Botto M. Are anti-C1q antibodies different from other SLE autoantibodies? Nat Rev Rheumatol 2010;6:490-3

70 Siegert CE, Daha MR, Swaak AJ, van der Voort EA, Breedveld FC. The relationship between serum titers of autoantibodies to C1q and age in the general population and in patients with systemic lupus erythematosus. Clin Immunol Immunopathol 1993;67:204-209.

71 Horvath L, Czirjak L, Fekete B, Jakab L, Pozsonyi T, Kalabay K, et al. High levels of antibodies against C1q are associated with disease activity and nephritis but not with other organ manifestations in SLE patients. Clin Exp Rheumatol 2001;19:667-672.

72 Moroni G, Trendelenburg M, Del Papa N, Quaglini S, Raschi E, Panzeri P, et al. Anti-C1q antibodies may help in diagnosing a renal flare in lupus nephritis. Am J Kidney Dis 2001;37: 490-498.

73 Grootscholten C, Dieker JW, McGrath FD, Roos A, Derksen RH, van der Vlag J, et al. A prospective study of anti-chromatin and anti-C1q autoantibodies in patients with proliferative lupus nephritis treated with cyclophosphamide pulses or azathioprine/methylprednisolone. Ann Rheum Dis 2007;66:693-696.

74 Moroni G, Radice A, Giammarresi G, Quaglini S, Gallelli B, Leoni A, et al. Are laboratory tests useful for monitoring the activity of lupus nephritis? A 6-year prospective study in a cohort of 228 patients with lupus nephritis, Ann Rheum Dis 2009;68:234-237.

75 Trouw LA, Groeneveld TW, Seelen MA, Duijs JM, Bajema IM, Prins FA, et al. Anti-C1q autoantibodies deposit in glomeruli but are only pathogenic in combination with glomerular C1q-containing immune complexes. J Clin Invest 2004;114:679-688.

76 Mannik M, Merrill CE, Stamps LD, Wener MH. Multiple autoantibodies form the glomerular immune deposits in patients with systemic lupus erythematosus. J Rheumatol 2003;30:1495-1504.

77 Bariety J, Bruneval P, Meyrier A, Mandet C, Hill G, Jacquot C, Podocyte involvement in human immune crescentic glomerulonephritis. Kidney Int 2005;68:1109-1119.

78 Sato Y, Wharram B, Lee SK, Wickman L, Goyal M, Venkatareddy M, Chang JW, Wiggins JE, Lienczewski C, Kretzler M, Wiggins RC. Urine podocyte mRNAs mark progression of renal disease. J Am Soc Nephrol 2009;20:1041-1052.

79 Bruschi M, Sinico RA, Moroni G, Pratesi F, Migliorini P, Galetti M, et al. Glomerular autoimmune multicomponents of human lupus nephritis in vivo: a-enolase and annexin AI. J Am Soc Nephrol 2013;25:2483-2498.

80 Bruschi M, Galetti M, Sinico RA, Moroni G, Bonanni A, Radice A, Tincani A, et al. Glomerular autoimmune multicomponents of human lupus nephritis in vivo (2): planted antigens. J Am Soc Nephrol 2015;26:1905-1924.

81 Thebault S, Gilbert D, Hubert M, Drouot L, Machour N, Lange C, et al. Orderly pattern of development of the autoantibody response in NZB/NZW F1 mice: characterization of target antigens and antigen spreading by two dimensional gel electrophoresis and mass spectrometry, J. Immunol 2002;169:4046-4053.

82 Kramers C, Hylkema MN, van Bruggen MC, van de Lagemaat R, Dijkman HB, Assmann KJ, Smeenk RJ, Berden JH. Anti-nucleosome antibodies complexed to nucleosomal antigens show anti-DNA reactivity and bind to rat glomerular basement membrane in vivo. J Clin Invest 1994;94:568-77.

83 van Bruggen MC, Walgreen B, Rijke TP, Corsius MJ, Assmann KJ, Smeenk RJ, van Dedem GW, Kramers K, Berden JH. Heparin and heparinoids prevent the binding of immune complexes containing nucleosomal antigens to the GBM and delay nephritis in MRL/lpr mice. Kidney Int 1996;50:1555-64.

84 Seredkina N, Rekvig OP. Acquired loss of renal nuclease activity is restricted to DNaseI and is an organ-selective feature in murine lupus nephritis. Am J Pathol 2011;179:1120-8.

85 Fenton K, Fismen S, Hedberg A, Seredkina N, Fenton C, Mortensen ES, et al. AntidsDNA antibodies promote initiation, and acquired loss of renal DNase1 promotes progression of lupus nephritis in autoimmune (NZB×NZW)F1 mice. PLoS One 2009;4:e8474.

86 Pedersen HL, Horvei KD, Thiyagarajan D, Norby GE, Seredkina N, Moroni G, Eilertsen GØ, Holdaas H, Strøm EH, Bakland G, Meroni PL, Rekvig OP. Lupus nephritis: low urinary DNase I levels reflect loss of renal DNase I and may be utilized as a biomarker of disease progression. J Pathol Clin Res 2018;4:193-203

87 Gatto M, Iaccarino L, Ghirardello A, Bassi N, Pontisso P, Punzi L, Shoenfeld Y, Doria A. Serpins, immunity and autoimmunity: old molecules, new functions. Clin Rev Allergy Immunol 2013;45:267-80.

88 Vidalino L, Doria A, Quarta S, Zen M, Gatta A, Pontisso P. SERPINB3, apoptosis and autoimmunity. Autoimmun Rev 2009;9:108–12.

89 Vidalino L, Doria A, Quarta SM, Crescenzi M, Ruvoletto M, Frezzato F, et al. SERPINB3 expression on B-cell surface in autoimmune diseases and hepatitis C virus-related chronic liver infection. Exp Biol Med 2012;237:793–802.

90 Suminami Y, Nagashima S, Vujanovic NL, Hirabayashi K, Kato H, Whiteside TL. Inhibition of apoptosis in human tumour cells by the tumour-associated serpin, SCC antigen-1. Br J Cancer 2000;82:981–9.

91 Turato C, Vitale A, Fasolato S, Ruvoletto M, Terrin L, Quarta S, et al. SERPINB3 is associated with TGF-b1 and cytoplasmic b-catenin expression in hepatocellular carcinomas with poor prognosis. Br J Cancer 2014;110:2708-15.

92 Ciscato F, Sciacovelli M, Villano G, Turato C, Bernardi P, Rasola A, et al. SERPINB3 protects from oxidative damage by chemotherapeutics through inhibition of mitochondrial respiratory complex I. Oncotarget 2013;5:2418–27.

93 Murakami A, Suminami Y, Hirakawa H, Nawata S, Numa F, Kato H. Squamous cell carcinoma antigen suppresses radiation-induced cell death. Br J Cancer 2001;84:851–8.

94 Garlanda C, Jaillon S, Doni A, Bottazzi B, Mantovani A. PTX3, a humoral pattern recognition molecule at the interface between microbe and matrix recognition. Curr Opin Immunol 2016;38:39–44.

95 Bottazzi B, Vouret-Craviari V, Bastone A, De Gioia L, Matteucci C, Peri G, et al. Multimer formation and ligand recognition by the long pentraxin PTX3. Similarities and differences with the

short pentraxins C-reactive proteinand serum amyloid P component. J Biol Chem 1997;72:32817–23.

96 Bottazzi B, Doni A, Garlanda C,Mantovani A. An integrated view of humoral innate immunity: pentraxins as a paradigm. Annu Rev Immunol 2010;28:157–83.

97 Doni A, Garlanda C, Bottazzi B, Meri S, Garred P, Mantovani A. Interactions of the humoral pattern recognition molecule PTX3 with the complement system. Immunobiology 2012;1122-8.

98 Inforzato A, Baldock C, Jowitt TA, Holmes DF, Lindstedt R, Marcellini M,et al. The angiogenic inhibitor long pentraxin PTX3 forms an asymmetric octamer with two binding sites for FGF2. J Biol Chem 2010;285:17681-92.

99 Baruah P, Propato A, Dumitriu IE, Rovere-Querini P, Russo V, Fontana R, et al. The pattern recognition receptor PTX3 is recruited at the synapse between dying and dendritic cells, and edits the cross-presentation of self, viral, and tumor antigens. Blood 2006;107:151-8.

100 Rovere P, Peri G, Fazzini F, Bottazzi B, Doni A, Bondanza A, Zimmermann VS, Garlanda C, Fascio U, Sabbadini MG, Rugarli C, Mantovani A, Manfredi AA. The long pentraxin PTX3 binds to apoptotic cells and regulates their clearance by antigen-presenting dendritic cells. Blood 2000;96:4300-6.

101 Chorny A, Chorny A, Casas-Recasens S, Sintes J, Shan M, Polentarutti N, García-Escudero R, et al. The soluble pattern recognition receptor PTX3 links humoral innate and adaptive immune responses by helping marginal zone B cells. J Exp Med 2016;213:2167-85.

102 de Oliveira THC, Souza DG, Teixeira MM, Amaral FA. Tissue Dependent Role of PTX3 During Ischemia-Reperfusion Injury. Front Immunol 2019;10;10:1461.

103 Ma YJ and Garred P (2018) Pentraxins in Complement Activation and Regulation. Front. Immunol 9:3046.

104 Nauta A, Bottazzi B, Mantovani A, Salvatori G, Kishore U, Schwaeble W, et al. Biochemical and functional characterization of the interaction between pentraxin 3 and C1q, Eur J Immunol 2003;33:465-473.

105 Bally I, Inforzato A, Dalonneau F, Stravalaci M, Bottazzi B, Gaboriaud C, Thielens NM. Interaction of C1q With Pentraxin 3 and IgM Revisited: Mutational Studies With Recombinant C1q Variants. Front Immunol 2019;10:461.

106 Bussolati B, Peri G, Salvidio G, Verzola D, Mantovani A, Camussi G. The long pentraxin PTX3 is synthesized in IgA glomerulonephritis and activates mesangial cells. J Immunol 2003;170:1466–72.

107 Nauta AJ, de Haij S, Bottazzi B, Mantovani A, Borrias MC, Aten J, et al. Human renal epithelial cells produce the long pentraxin PTX3. Kidney Int 2005;67:543–553.

108 Bassi N, Ghirardello A, Blank M, Zampieri S, Sarzi-Puttini P, Mantovani A, Doria A. IgG anti-pentraxin 3 antibodies in systemic lupus erythematosus. Ann Rheum Dis 2010 69 1704-1710.

109 Yuan M, Tan Y, Pang Y, Li YZ, Song Y, Yu F, et al. Anti-pentraxin 3 autoantibodies might be protective in lupus nephritis: a large cohort study. Ren Fail 2017;39:465–73.

110 Bassi N, Del Prete D,Ghirardello A, Gatto M, Ceol M, Zen M, et al. PTX3, anti-PTX3, and anti-C1q autoantibodies in lupus glomerulonephritis. Clin Rev Allergy Immunol 2015;49:217-226.

111 Pang Y, Tan Y, Li Y, Zhang J, Guo Y, Guo Z, et al. Pentraxin 3 Is Closely Associated With Tubulointerstitial Injury in Lupus Nephritis: A Large Multicenter Cross-Sectional Study. Medicine (Baltimore) 2016;95:e2520.

112 Li W, Titov A, Morel L. An update on lupus animal models. CurrOpin Rheumatol (2017) 29:434–41.

113 Hochberg MC. Updating the American College of Rheumatology revised criteria for the classification of systemic lupus erythematosus. Arthritis Rheum 1997; 40: 1725

114 Moroni G, Vercelloni PG, Quaglini S, Gatto M, Gianfreda D, Sacchi L, Raffiotta F, Zen M, Costantini G, Urban ML, Pieruzzi F, Messa P, Vaglio A, Sinico RA, Doria A. Changing patterns in clinical-histological presentation and renal outcome over the last five decades in a cohort of 499 patients with lupus nephritis. Ann Rheum Dis 2018;77:1318-1325.

115 Beccati M, Martini V, Comazzi S, Fanton N, Cornegliani L. Lymphocyte subpopulations and Treg cells in dogs with atopic dermatitis receiving ciclosporin therapy: a prospective study. Vet Dermatol 2016;27:17-e5.

116 Gelain ME, Mazzilli M, Riondato F, Marconato L, Comazzi S. Aberrant phenotypes and quantitative antigen expression in different subtypes of canine lymphoma by flow cytometry. Vet Immunol Immunopathol 2008;121:179-88.

117 Bardwell PD, Gu J, McCarthy D, Wallace C, Bryant S, Goess C, et al. The Bcl-2 family antagonist ABT-737 significantly inhibits multiple animal models of autoimmunity. J Immunol 2009;182:7482–89.

118 Berkowska MA, Driessen GJ, Bikos V, Grosserichter-Wagener C, Stamatopoulos K, Cerutti A, et al. Human memory B cells originate from three distinct germinal center-dependent and -independent maturation pathways. Blood 2011;118:2150–8.

119 Dillard MG, Tillman RL, Sampson CC. Lupus Nephritis. Correlations between the clinical course and presence of electron-dense deposits. Lab Invest 1975;32:261-9.

120 Sjöwall C, Olin AI, Skogh T, Wetterö J, Mörgelin M, Nived O, Sturfelt G, Bengtsson AA. C-reactive protein, immunoglobulin G and complement co-localize in renal immune deposits of proliferative lupus nephritis. Autoimmunity 2013;46:205-14.

121 Zhang J, Jacobi AM, Wang T, Berlin R, Volpe BT, Diamond B. Polyreactive autoantibodies in systemic lupus erythematosus have pathogenic potential. J Autoimmun 2009;33:270-4.

122 Tipton CM, Fucile CF, Darce J, Chida A, Ichikawa T, Gregoretti I, et al. Diversity, cellular origin and autoreactivity of antibody-secreting cell population expansions in acute systemic lupus erythematosus. Nat Immunol 2015;16:755-65.

123 Weller S, Braun MC, Tan BK, Rosenwald A, Cordier C, Conley ME, et al. Human blood IgM "memory" B cells are circulating splenic marginal zone B cells harboring a prediversified immunoglobulin repertoire. Blood 2004;104:3647-54.

124 Weller S, Mamani-Matsuda M, Picard C, Cordier C, Lecoeuche D, Gauthier F, Weill JC, Reynaud CA. Somatic diversification in the absence of antigen-driven responses is the hallmark of the IgM+ IgD+ CD27+ B cell repertoire in infants. J Exp Med 2008;205:1331-42.

125 Budeus B, Schweigle de Reynoso S, Przekopowitz M, Hoffmann D, Seifert M, Küppers R. Complexity of the human memory B-cell compartment is determined by the versatility of clonal diversification in germinal centers. Proc Natl Acad Sci USA 2015;112:E5281-9.